

Bayesian Inference of Infected Patients in Group Testing with Prevalence Estimation

Ayaka Sakata*

Institute of Statistical Mathematics, 10-3 Midori-cho, Tachikawa, Tokyo 190-8562, Japan

*Department of Statistical Science, The Graduate University for Advanced Science (SOKENDAI), Hayama-cho, Kanagawa 240-0193, Japan and
JST PRESTO, 4-1-8 Honcho, Kawaguchi, Saitama, 332-0012, Japan*

Group testing is a method of identifying infected patients by performing tests on a pool of specimens collected from patients. For the case in which the test returns a false result with finite probability, Bayesian inference and a corresponding belief propagation (BP) algorithm are introduced to identify the infected patients from the results of tests performed on the pool. It is shown that the true-positive rate is improved by taking into account the credible interval of a point estimate of each patient. Further, the prevalence and the error probability in the test are estimated by combining an expectation-maximization method with the BP algorithm. As another approach, a hierarchical Bayes model is introduced to identify the infected patients and estimate the prevalence. By comparing these methods, a guide for practical usage is formulated.

I. INTRODUCTION

In clinical testing methods such as blood tests and polymerase chain reaction (PCR) tests, discovering infected patients from a large population requires significant operating costs. Because of limitations in the number of available devices, reagents, and technologists, a high demand exists for more efficient methods of testing. Group testing is one of the approaches for the reduction of the operating costs by performing tests on pools of specimens obtained from patients [1, 2]. It is known that if the rate of the infected patients in the population is sufficiently small, in principle, one can identify the infected patients from the tests on pools whose number is smaller than that of the population. Originally, group testing was developed for blood testing during World War II, and is now applied to various fields such as quality control in product testing [3], estimation of the content of genetically mutated organisms in maize grains [4], and multiple access communication [5].

The identification of the infected patients from the results of group test is mathematically formulated as a channel coding problem to reconstruct the original signal from a codeword transferred through noisy channel [6], where the original signal, codeword, and noisy channel correspond to the state of patients, states of the pools, and errors in the tests, respectively. Further, group testing can be regarded as a variant of compressed sensing [7, 8] with discrete variables and logical sums. Hence, the progress in the last decade in sparse estimation including compressed sensing has revived interest in group testing, and information-theory approaches have achieved bound evaluation of group testing at a limiting case [9, 10].

Recently, in response to the epidemic infection of COVID-19 that requires testing on large populations, the idea of group testing has attracted increasing attention [11–13] from the viewpoint of practical application rather than mathematics. In practice, clinical testing sometimes results in errors even when the operation is precise. For example, in PCR tests, false negative probabilities of up to 3% and false positive (FP) probabilities of up to 5% have been observed [14]. Moreover, the bacterial or viral load in the specimen depends on the specimen collection method and timing [15]. Therefore, a specimen sometimes does not contain a sufficient amount of the pathogen to exceed the detection limit, even when the patient is infected. Further, post-collection contamination of pathogens into a specimen can cause a positive result even when the patient is not infected. Statistical inference can contribute to the correction of errors by estimating the true state of patients from noisy test data, and quantifying the credibility of the estimation.

In this paper, Bayesian inference is introduced to identify the infected patients in the group testing problem considering the finite false probabilities in the test. The infection probability of each patient is approximately calculated by a belief propagation (BP) algorithm because of its low computational cost [16], although the BP algorithm does not achieve the information theoretic bound [10]. Our contributions with regard to the BP algorithm are as follows:

- : (i) The true positive (TP) ratio, namely the ratio of infected patients reconstructed as positive, is improved to be greater than the TP probability in the test by considering the confidence interval of the point estimate, corresponding to the infection probability. A bootstrap method is introduced to construct the confidence interval.
- : (ii) In our framework, prevalence, which is the fraction of the infected patients in the population, is introduced into the prior distribution of the patients' state. Prevalence is one of the fundamental measures in epidemiology, and group testing

* ayaka@ism.ac.jp

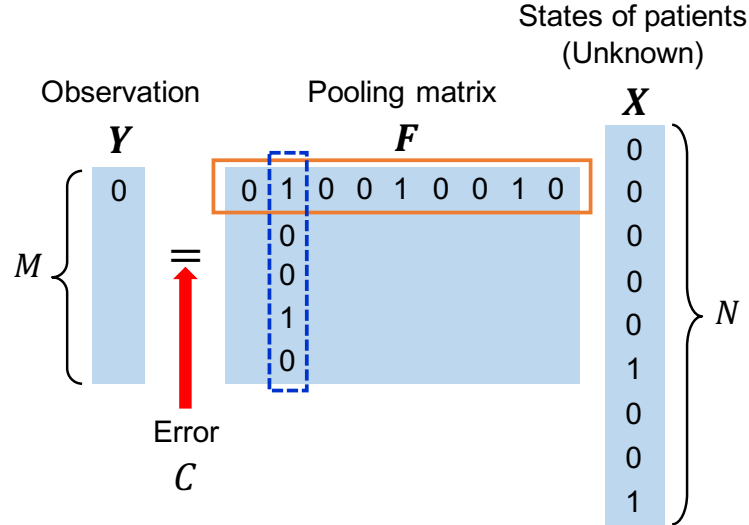


FIG. 1. Matrix representation of group testing, where each pool size is $N_G = 3$ and each overlap is $N_O = 2$. The summation in the usual matrix product is replaced with a logical sum.

has been applied to its estimation [17–19]. The estimator of prevalence is constructed in addition to the identification of the infected patients by combining an expectation-maximization (EM) method with a BP algorithm. Following the same procedure, the TP and FP probabilities of the test are estimated.

- (iii) As another approach, the hierarchical Bayes model is introduced to identify the infected patients and estimate the prevalence. BP algorithm is applied to the hierarchical Bayes model and evaluate the performance in comparison with the approach described in (ii), and observe that the computational cost of the hierarchical Bayes approach is lower than that required in (ii).

The remainder of the paper is organized as follows. In Section II, the problem setting of group testing is explained and introduce Bayesian inference. In Section III, the BP algorithm is introduced and show its reconstruction performance under finite false probabilities. In Section IV, an estimator based on the confidence interval of the estimated infection probability is proposed. In Section V, the estimation of the unknown parameters in group testing is discussed by using the likelihood calculated by the BP algorithm. In Section VI, the hierarchical Bayes model for group testing is introduced and discuss the estimation of the prevalence by applying the BP algorithm to the hierarchical model. Section VII presents a summary and discussion.

II. PROBLEM SETTING

We consider a population of N patients and M groups on which the test is performed. Let us denote the state of N -patients by $\mathbf{X}^{(0)} \in \{0, 1\}^N$, where $X_i = 1$ and $X_i = 0$ means that i -th patient is infected and not infected, respectively. The grouping of the patients is determined by the pooling matrix $\mathbf{F} \in \{0, 1\}^{M \times N}$, where $F_{\mu i} = 1$ and $F_{\mu i} = 0$ means that the i -th patient is in the μ -th group and not, respectively. The true state of the μ ($= 1, \dots, M$)-th group, denoted by $Y_\mu^{(0)}$, is given by

$$Y_\mu^{(0)} = \bigvee_{i=1}^N F_{\mu i} X_i^{(0)}, \quad (1)$$

where $\bigvee_{i=1}^N f_i = f_1 \vee f_2 \vee \dots \vee f_N$ denotes the logical sum of N components. Namely, when μ -th pool contains at least one infected patient, the state of the μ -th pool is 1 (positive), and 0 (negative) otherwise.

The test returns a false result with finite probability. We assume that the errors in the tests are independent from each other and model the observation (result of the test) as

$$Y_\mu = C\left(\bigvee_{i=1}^N F_{\mu i} X_i^{(0)}\right), \quad (2)$$

where $C(\cdot)$ is the probabilistic function whose behavior is given by [10]

$$P(C(a) = 1|a = 1) = p_{\text{TP}}, \quad P(C(a) = 0|a = 1) = 1 - p_{\text{TP}} \quad (3)$$

$$P(C(a) = 1|a = 0) = p_{\text{FP}}, \quad P(C(a) = 0|a = 0) = 1 - p_{\text{FP}}. \quad (4)$$

Here, p_{TP} and p_{FP} correspond to the TP and FP probabilities in the test, respectively, and these values are common for all tests. Fig.1 shows matrix representation of the group testing, where the summations in the usual matrix factorization are replaced with a logical sum. We focus on the case $\alpha \equiv M/N < 1$, where the number of tests is smaller than that of the patients. Hereafter, we consider that the size of group is fixed to N_G . Further, the overlap, which is the number of groups that each patient belongs to, is fixed at N_O ; hence, the relationship $N_O = \alpha \times N_G$ holds.

A. Bayesian inference

From the property of $C(\cdot)$, the generative model of \mathbf{Y} is given by

$$P(\mathbf{Y}|\mathbf{X}^{(0)}, p_{\text{TP}}, p_{\text{FP}}) = \prod_{\mu=1}^M P(Y_{\mu}|\mathbf{X}^{(0)}, p_{\text{TP}}, p_{\text{FP}}) \quad (5)$$

where

$$\begin{aligned} P(Y_{\mu}|\mathbf{X}, p_{\text{TP}}, p_{\text{FP}}) &= p_{\text{TP}}Y_{\mu}T_{\mu}(\mathbf{X}^{(0)}) + (1 - p_{\text{TP}})(1 - Y_{\mu})T_{\mu}(\mathbf{X}^{(0)}) \\ &+ p_{\text{FP}}Y_{\mu}(1 - T_{\mu}(\mathbf{X}^{(0)})) + (1 - p_{\text{FP}})(1 - Y_{\mu})(1 - T_{\mu}(\mathbf{X}^{(0)})), \end{aligned} \quad (6)$$

and $T_{\mu}(\mathbf{X}^{(0)}) = \prod_{i=1}^{N_G} F_{\mu i} X_i^{(0)}$. The purpose is to infer the true states of patients $\mathbf{X}^{(0)}$ from the observation \mathbf{Y} .

In general, the true generative process of \mathbf{Y} is unknown, but it is reasonable to assume that the process is expressed by the conditional Bernoulli distribution eq.(5), as the variables \mathbf{Y} and $\mathbf{X}^{(0)}$ are binary, although the value of true parameters p_{TP} and p_{FP} are not known in advance. Bayesian inference is a preferred method in the presence of the reasonable model. As prior distribution of the patient states, we use the following distribution:

$$P_0(\mathbf{X}|\rho) = \prod_{i=1}^N \{\rho X_i + (1 - \rho)(1 - X_i)\}, \quad (7)$$

where $\rho \in [0, 1]$ is the prevalence, which is not known in advance. The prevalence of the population does not necessarily match an individual's infection probability; hence, the prior distribution eq.(7) is an assumption. We consider that this form of prior information is appropriate for prevalence estimation as the prevalence of the population generated by Bernoulli(ρ) converges to ρ for sufficiently large N .

Following the Bayes rule, the posterior distribution is given by

$$P(\mathbf{X}|\mathbf{Y}) \propto P(\mathbf{Y}|\mathbf{X}, \hat{p}_{\text{TP}}, \hat{p}_{\text{FP}})P_0(\mathbf{X}|\hat{\rho}), \quad (8)$$

where \hat{p}_{TP} , \hat{p}_{FP} , and $\hat{\rho}$ are the assumed TP probability, FP probability, and prevalence, respectively. The i -th patient's state is identified on the basis of the marginal distribution given by

$$P(X_i|\mathbf{Y}) = \sum_{\mathbf{X} \setminus X_i} P(\mathbf{X}|\mathbf{Y}) \quad (9)$$

where $\mathbf{X} \setminus X_i$ denotes the components of \mathbf{X} other than X_i . As the variable X_i is binary, we can represent the marginal distribution using a Bernoulli probability θ_i as

$$P(X_i|\mathbf{Y}) = \theta_i X_i + (1 - \theta_i)(1 - X_i), \quad (10)$$

and θ_i corresponds to the infection probability, namely, the probability that $X_i = 1$. The simplest estimate of $X_i^{(0)}$ is the maximum a posteriori (MAP) estimator given by

$$X_i^{(\text{MAP})} = \mathbb{I}(\theta_i > 0.5), \quad (11)$$

where $\mathbb{I}(a)$ is the indicator function whose value is 1 when a is true, and 0 otherwise.

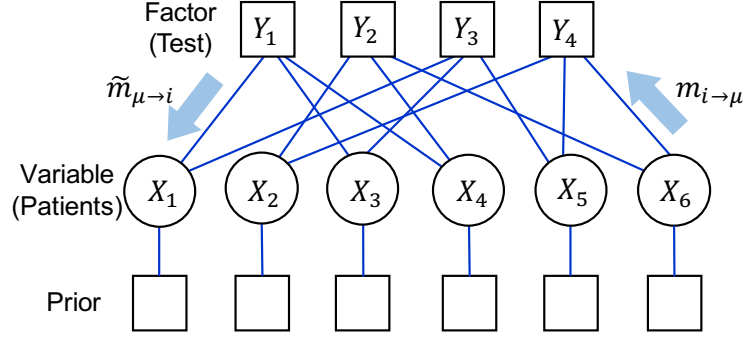


FIG. 2. Factor graph representation of group testing for $N = 6$, $M = 4$, $N_G = 3$, and $N_O = 2$.

III. BELIEF PROPAGATION

The computation of the marginal distribution requires an exponential order of the sums, and is thus intractable. We approximately calculate the marginal distribution using the BP algorithm on the factor graph representation of the group testing [10, 20]. Comparing the approximation by BP algorithm with the exact calculation at a small size such as $N = 20$, we find that the accuracy of the BP algorithm is sufficient for applying it to the group testing problem (see Appendix A). As another numerical approach, Markov chain Monte Carlo (MCMC) method can be applied to the current problem setting; however, MCMC requires high computational cost and is not feasible particularly for estimating the unknown parameter, as discussed in Section V. In this study, we use the BP algorithm as a reasonable method owing to its approximation accuracy and computational time.

Fig. 2 shows the factor graph representation of the group testing for $N = 6$, $M = 4$, $N_G = 3$, and $N_O = 2$. Here, $\mathcal{M}(\mu)$ and $\mathcal{G}(i)$ denote the indices of the patients in the μ -th pool, and those of the pools in which the i -th patient is included, respectively. The conditional probability $P(Y_\mu | \mathbf{X})$ depends on X_i ($i \in \mathcal{M}(\mu)$); hence, the posterior distribution can be expressed as a bipartite graph, as shown in Fig. 2. For the edge that connects the μ -th factor (test) and the i -th variable (patient), two types of messages are defined as

$$\tilde{m}_{\mu \rightarrow i}(X_i) \propto \sum_{\mathbf{X} \setminus X_i} P(Y_\mu | \mathbf{X}, \hat{p}_{\text{TP}}, \hat{p}_{\text{FP}}) \prod_{j \in \mathcal{M}(\mu) \setminus i} m_{j \rightarrow \mu}(X_j) \quad (12)$$

$$m_{i \rightarrow \mu}(X_i) \propto P_0(X_i | \hat{\rho}) \prod_{v \in \mathcal{G}(i) \setminus \mu} \tilde{m}_{v \rightarrow i}(X_i), \quad (13)$$

which correspond to posterior information and output information, respectively. Intuitively, the messages $m_{i \rightarrow \mu}(X_i)$ and $\tilde{m}_{\mu \rightarrow i}(X_i)$ represent the marginal distributions of X_i before and after the μ -th test is performed, respectively. As $X_i \in \{0, 1\}$, these messages are represented by one parameter as

$$\tilde{m}_{\mu \rightarrow i}(X_i) = \tilde{\theta}_{\mu \rightarrow i} X_i + (1 - \tilde{\theta}_{\mu \rightarrow i})(1 - X_i) \quad (14)$$

$$m_{i \rightarrow \mu}(X_i) = \theta_{i \rightarrow \mu} X_i + (1 - \theta_{i \rightarrow \mu})(1 - X_i), \quad (15)$$

where $\tilde{\theta}_{\mu \rightarrow i}$ and $\theta_{i \rightarrow \mu}$ are given by

$$\tilde{\theta}_{\mu \rightarrow i} = \frac{U_\mu}{\tilde{Z}_{\mu \rightarrow i}} \quad (16)$$

$$\theta_{i \rightarrow \mu} = \frac{\hat{\rho} \prod_{v \in \mathcal{G}(i) \setminus \mu} \tilde{\theta}_{v \rightarrow i}}{Z_{i \rightarrow \mu}} \quad (17)$$

and

$$U_\mu = p_{\text{TP}} Y_\mu + (1 - p_{\text{TP}})(1 - Y_\mu) \quad (18)$$

$$W_\mu = p_{\text{FP}} Y_\mu + (1 - p_{\text{FP}})(1 - Y_\mu) \quad (19)$$

$$\tilde{Z}_{\mu \rightarrow i} = U_\mu \left(2 - \prod_{j \in \mathcal{M}(\mu) \setminus i} (1 - \theta_{j \rightarrow \mu}) \right) + W_\mu \prod_{j \in \mathcal{M}(\mu) \setminus i} (1 - \theta_{j \rightarrow \mu}) \quad (20)$$

$$Z_{i \rightarrow \mu} = \hat{\rho} \prod_{v \in \mathcal{G}(i) \setminus \mu} \tilde{\theta}_{v \rightarrow i} + (1 - \hat{\rho}) \prod_{v \in \mathcal{G}(i) \setminus \mu} (1 - \tilde{\theta}_{v \rightarrow i}). \quad (21)$$

Using these messages, we can approximate the marginal distribution as

$$\begin{aligned} P(X_i) &\propto \{\hat{\rho}X_i + (1 - \hat{\rho})(1 - X_i)\} \prod_{\mu \in \mathcal{G}(i)} \tilde{m}_{\mu \rightarrow i}(X_i) \\ &= \left(\hat{\rho} \prod_{\mu \in \mathcal{G}(i)} \tilde{\theta}_{\mu \rightarrow i} \right) X_i + \left((1 - \hat{\rho}) \prod_{\mu \in \mathcal{G}(i)} (1 - \tilde{\theta}_{\mu \rightarrow i}) \right) (1 - X_i), \end{aligned} \quad (22)$$

and thus the infection probability is approximated as

$$\hat{\theta}_i = \frac{\hat{\rho} \prod_{\mu \in \mathcal{G}(i)} \tilde{\theta}_{\mu \rightarrow i}}{\hat{\rho} \prod_{\mu \in \mathcal{G}(i)} \tilde{\theta}_{\mu \rightarrow i} + (1 - \hat{\rho}) \prod_{\mu \in \mathcal{G}(i)} (1 - \tilde{\theta}_{\mu \rightarrow i})}, \quad (23)$$

and the MAP estimator is given by

$$\hat{X}_i^{(MAP)} = \mathbb{I}(\hat{\theta}_i > 0.5). \quad (24)$$

Algorithm 1 BP for Bayesian Group Testing

Input: $Y \sim P(Y|X^{(0)})$ and F

Output: $\theta \in [0, 1]^N$

- 1: $\{\theta_{i \rightarrow \mu}^{(0)}\} \leftarrow$ initial values from $[0, 1]^{N \times M}$
 - 2: $\{\tilde{\theta}_{\mu \rightarrow i}^{(0)}\} \leftarrow$ initial values from $[0, 1]^{M \times N}$
 - 3: $U \leftarrow p_{TP}Y + (1 - p_{TP})(\mathbf{1}_M - Y)$
 - 4: $W \leftarrow p_{FP}Y + (1 - p_{FP})(\mathbf{1}_M - Y)$
 - 5: **for** $t = 1 \dots T$ **do**
 - 6: **for** all combinations of (μ, i) such that $F_{\mu i} = 1$ **do**
 - 7: $\tilde{Z}_{\mu \rightarrow i}^{(t)} \leftarrow U_{\mu} \left\{ 2 - \prod_{j \in \mathcal{M}(\mu) \setminus i} (1 - \theta_{j \rightarrow \mu}^{(t-1)}) \right\} + W_{\mu} \prod_{j \in \mathcal{M}(\mu) \setminus i} (1 - \theta_{j \rightarrow \mu}^{(t-1)})$
 - 8: $Z_{i \rightarrow \mu}^{(t)} \leftarrow \rho \prod_{\nu \in \mathcal{G}(i) \setminus \mu} \tilde{\theta}_{\nu \rightarrow i}^{(t-1)} + (1 - \rho) \prod_{\nu \in \mathcal{G}(i) \setminus \mu} (1 - \tilde{\theta}_{\nu \rightarrow i}^{(t-1)})$
 - 9: $\tilde{\theta}_{\mu \rightarrow i}^{(t)} \leftarrow \frac{U_{\mu}}{\tilde{Z}_{\mu \rightarrow i}^{(t)}}$
 - 10: $\theta_{i \rightarrow \mu}^{(t)} \leftarrow \frac{\rho \prod_{\nu \in \mathcal{G}(i) \setminus \mu} \tilde{\theta}_{\nu \rightarrow i}^{(t-1)}}{Z_{i \rightarrow \mu}^{(t)}}$
 - 11: **end for**
 - 12: **end for**
 - 13: **for** $i = 1 \dots N$ **do**
 - 14: $\hat{\theta}_i \leftarrow \frac{\rho \prod_{\mu \in \mathcal{G}(i)} \tilde{\theta}_{\mu \rightarrow i}^{(T)}}{\rho \prod_{\mu \in \mathcal{G}(i)} \tilde{\theta}_{\mu \rightarrow i}^{(T)} + (1 - \rho) \prod_{\mu \in \mathcal{G}(i)} (1 - \tilde{\theta}_{\mu \rightarrow i}^{(T)})}$
 - 15: **end for**
-

First, we consider the case where we know the correct parameters; $\hat{p}_{TP} = p_{TP}$, $\hat{p}_{FP} = p_{FP}$, and $\hat{\rho} = \rho$. The pseudocode of the BP algorithm for group testing with known parameters is shown in Algorithm 1. We introduce a damping factor $d \in (0, 1]$ for the stabilization of the algorithm as

$$\tilde{\theta}_{\mu \rightarrow i}^{(t)} \leftarrow d\tilde{\theta}_{\mu \rightarrow i}^{(t-1)} + (1 - d)\tilde{\theta}_{\mu \rightarrow i}^{(t-2)} \quad (25)$$

$$\theta_{i \rightarrow \mu}^{(t)} \leftarrow d\theta_{i \rightarrow \mu}^{(t-1)} + (1 - d)\theta_{i \rightarrow \mu}^{(t-2)}. \quad (26)$$

In all the numerical simulations performed in this study, we set $d = 0.1$ conservatively; however, this choice extends the time for convergence. An adaptive setting of the damping factor for group testing is worth studying to achieve faster and stable convergence [21].

We check the performance of BP algorithm for randomly constructed pooling matrix under the constraint as $\sum_i F_{\mu i} = N_G \forall \mu$ and $\sum_{\mu} F_{\mu i} = N_O \forall i$. The true state of patients $X^{(0)}$ is also randomly generated under the constraint $\sum_i X_i^{(0)} = N\rho$. The accuracy

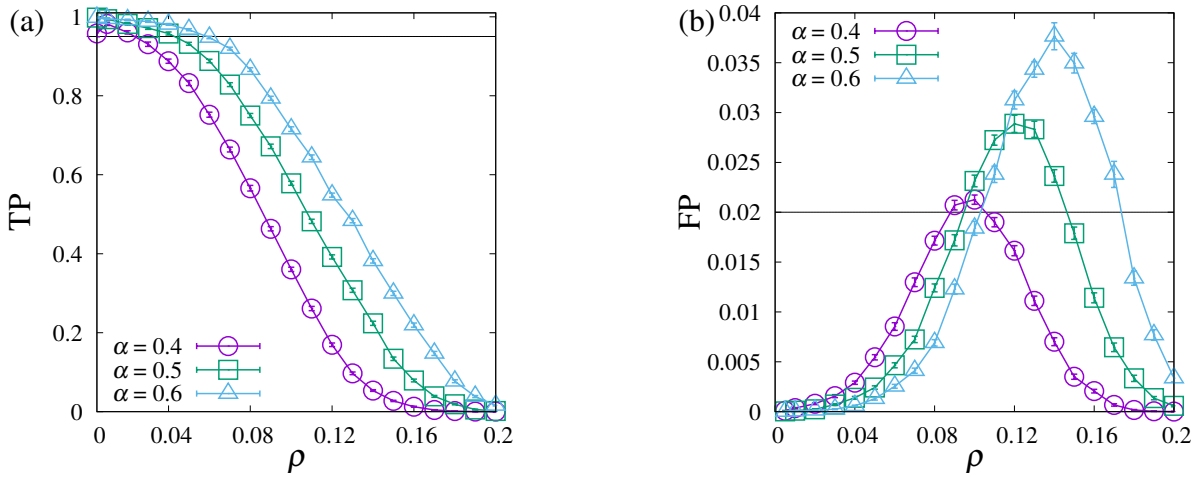


FIG. 3. ρ -dependence of (a) TP and (b) FP at $N = 1000$ and $N_G = 10$ for various $\alpha = M/N$. Error probabilities on the test are fixed at $p_{\text{TP}} = 0.95$ and $p_{\text{FP}} = 0.02$. The horizontal lines in (a) and (b) represent p_{TP} and p_{FP} , respectively.

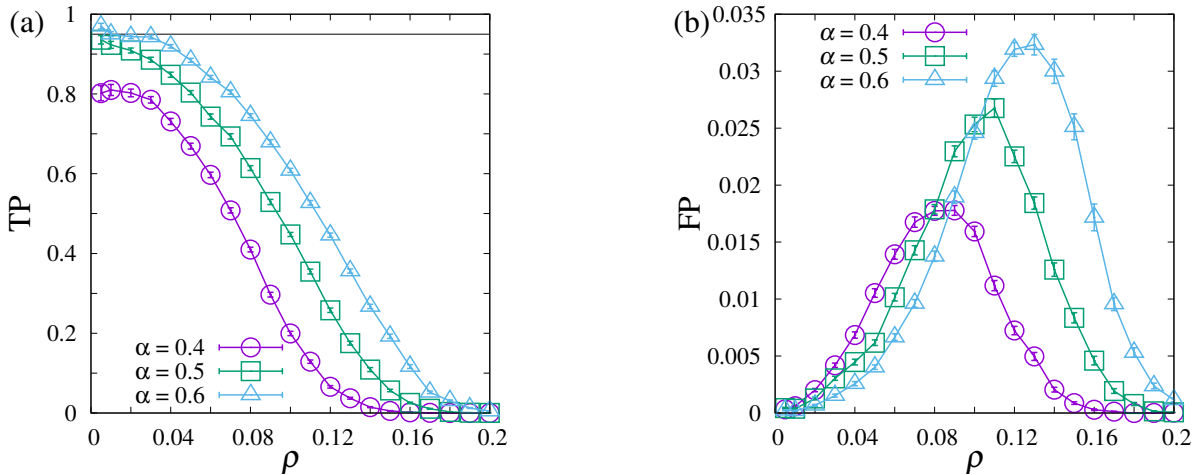


FIG. 4. ρ -dependence of (a) TP and (b) FP at $N = 1000$ and $N_G = 10$ for various α . Error rates are fixed at $p_{\text{TP}} = 0.95$ and $p_{\text{FP}} = 0.1$. The horizontal line in (a) represents p_{TP} . The FP region shown in (b) is below p_{FP} .

of the MAP estimator is measured using the TP rate and FP rate, given by

$$\text{TP} = \frac{\frac{1}{N} \sum_i X_i^{(0)} \hat{X}_i^{(\text{MAP})}}{\frac{1}{N} \sum_i X_i^{(0)}} \quad (27)$$

$$\text{FP} = \frac{\frac{1}{N} \sum_i (1 - X_i^{(0)}) \hat{X}_i^{(\text{MAP})}}{1 - \frac{1}{N} \sum_i X_i^{(0)}}, \quad (28)$$

respectively. A TP value larger than p_{TP} and an FP value smaller than p_{FP} indicate that the performance of the BP-based identification is better than the parallel test of N -patients. Fig.3 shows ρ -dependence of (a) TP and (b) FP at $N = 1000$, $N_G = 10$, $p_{\text{TP}} = 0.95$, and $p_{\text{FP}} = 0.02$, respectively. Each data point represents the averaged value with respect to 100 realizations of \mathbf{Y} and $\mathbf{X}^{(0)}$. The horizontal lines in (a) and (b) indicate 0.95 and 0.02, which are the TP and FP probabilities of the test, respectively. As α increases, that is, as the number of tests increases, TP increases and the ρ region where TP is larger than p_{TP} extends. FP also has a smaller value than p_{FP} for small values of ρ , and this success region extends as α increases. A similar tendency is shown for different values of p_{TP} and p_{FP} . As an example, we show the TP and FP for $N = 1000$, $N_G = 10$, $p_{\text{TP}} = 0.95$, and $p_{\text{FP}} = 0.1$ in Fig.4. The FP probability p_{FP} has significant influence on TP, which is evident from the comparison of Figs. 3 and 4. Intuitively, an increase in p_{FP} (or decrease in p_{TP}) causes uncertainty of the identification and decreases $\hat{\theta}_i$; hence, the MAP estimator tends to be zero.

As shown in Figs. 3 and 4, the TP and FP converge to zero as ρ increases. To understand this behavior, let us consider the

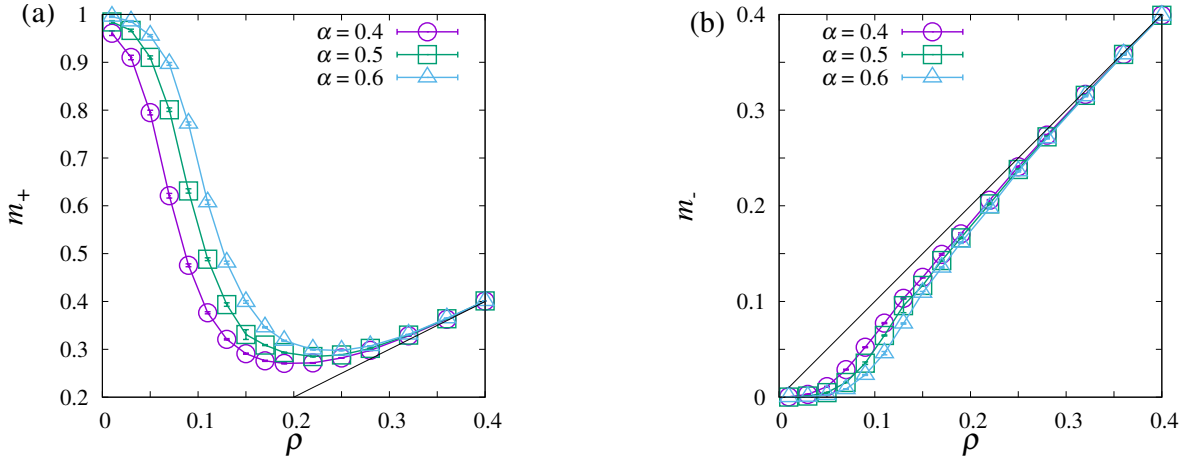


FIG. 5. ρ -dependence of (a) m_+ and (b) m_- at $N = 1000$ and $N_G = 10$ for various α . Error rates are fixed at $p_{TP} = 0.95$ and $p_{FP} = 0.02$. The gradients of solid lines are 1.

following quantities

$$m_+ = \frac{1}{N\rho} \sum_{i=1}^N X_i^{(0)} \hat{\theta}_i \quad (29)$$

$$m_- = \frac{1}{N(1-\rho)} \sum_{i=1}^N (1 - X_i^{(0)}) \hat{\theta}_i, \quad (30)$$

which correspond to the magnetization for infected patients and non-infected patients, respectively. Fig.5 shows the ρ -dependence of (a) m_+ and (b) m_- at $N = 1000$, $N_G = 10$, $p_{TP} = 0.95$, and $p_{FP} = 0.02$, which are the same parameters as those used for Fig.3. The values m_+ and m_- converge to ρ from above and from below, respectively, as ρ increases. This means that the infection probability $\hat{\theta}_i$ tends to be ρ without depending on the value $X_i^{(0)}$ at a sufficiently large ρ . Therefore, from the definition of the MAP estimator, $\hat{X}_i^{(\text{MAP})} = 0$ holds for any i , resulting in $TP = FP = 0$, when $\rho (< 0.5)$ is sufficiently large to be $m_+ \rightarrow \rho$ and $m_- \rightarrow \rho$. At $\rho \geq 0.5$, the estimate becomes $\hat{\theta}_i \rightarrow \rho \geq 0.5$ for any i ; hence, $\hat{X}_i^{(\text{MAP})} = 1$ holds and $TP = FP = 1$.

I note that the relationship $\hat{\theta}_i \rightarrow \rho$ is caused by the modeling and not the BP algorithm. In fact, the exact calculation of the posterior distribution and the corresponding MAP estimator achieve similar result, as shown in AppendixA. In the BP algorithm, $\hat{\theta}_i \rightarrow \rho$ is achieved by messages $\tilde{\theta}_{\mu \rightarrow i} \rightarrow 0.5$ and $\theta_{i \rightarrow \mu} \rightarrow \rho$ for any μ such that $F_{\mu i} = 1$. These messages indicate that the infection probability is determined by the prior distribution.

The dependence of the TP on p_{TP} and p_{FP} is shown in Fig.6(a) at $N = 1000$, $N_G = 10$ ($N_O = 5$), and $\rho = 0.01$. The solid line indicates $TP = p_{TP}$, and a TP value over the solid line means that the reconstruction by the BP algorithm achieves a higher TP than the parallel test of N -patients, and this situation is achieved at a sufficiently small FP probability $p_{FP} < 0.05$ in this parameter region. The reconstruction performance also depends on N_G . Fig.6 (b) shows the N_G -dependence of the TP at $N = 1000$, $M = 500$, $p_{TP} = 0.95$, and $p_{FP} = 0.05$. The TP increases as N_G increases without increasing the number of tests.

In practical testing, one of the objectives is to identify the infected patients to prevent the spread of the disease. Therefore, increasing the TP is a priority, and we mainly focus on the improvement of the TP using the BP algorithm.

A. BP algorithm needs “decision threshold”

Before proceeding to the improvement of the TP, we discuss the trivial fixed points of the BP algorithm and introduce the idea of “decision threshold” for the identification of infected patients.

From eq.(23), when $\tilde{\theta}_{\mu \rightarrow i} = 1$ for $\mu \in \mathcal{G}(i)$, we obtain $\hat{\theta}_i = 1$ irrespective of the value of ρ . This situation arises when $\theta_{j \rightarrow \mu} = 0$ for $j \in \mathcal{M}(\mu) \setminus i$ at $p_{FP} = 0$. Therefore, $\hat{\theta}_i = 1$ is achieved when the patients $j \in \mathcal{M}(\mu) \setminus i$ are estimated as negative before μ -th test is performed, where $\mu \in \mathcal{G}(i)$. This is the case in which the i -th patient is trivially identified as positive. In other words, the BP algorithm does not return $\hat{\theta}_i = 1$ for general cases; hence, to determine the infected patients $X_i^{(0)} \in \{0, 1\}$ from an estimate at the BP fixed point $\hat{\theta}_i \in [0, 1]$, we need a “decision threshold” such as a MAP estimator, where $\hat{\theta}_i = 0.5$ is the threshold for determining the infected patients. The TP and FP depend on this threshold, and our strategy for the improvement of TP is an appropriate threshold choice, as discussed in the next section.

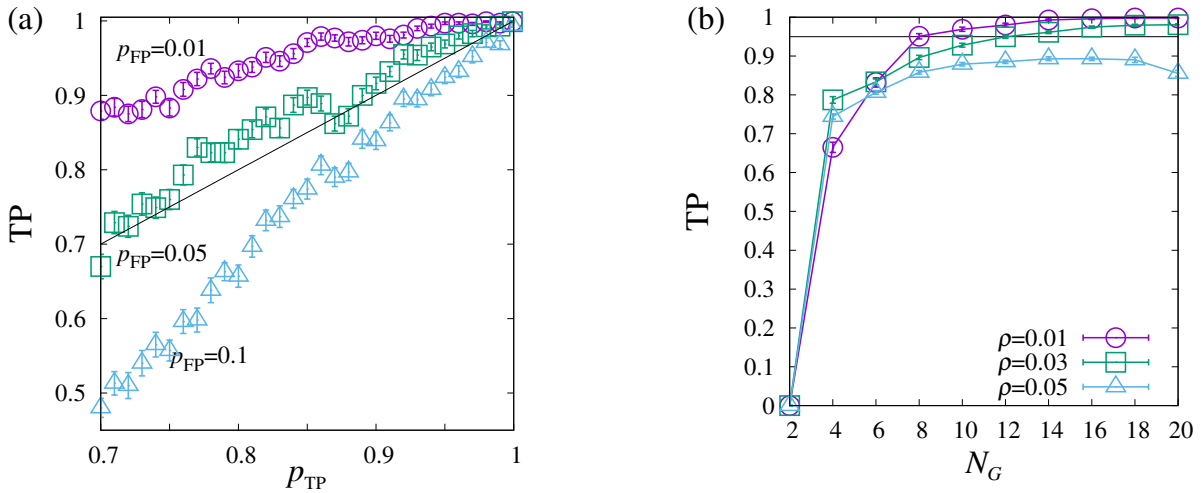


FIG. 6. (a) p_{TP} -dependence of TP at $N = 1000$, $M = 500$, $N_G = 10$ ($N_O = 5$), and $\rho = 0.01$ for different values of p_{FP} . (b) N_G -dependence of TP at $N = 1000$, $M = 500$ and $p_{TP} = 0.95$, $p_{FP} = 0.05$. The solid line indicates 0.95 (p_{TP}).

The threshold at $\hat{\theta}_i = 0$ is expected to obtain a conservative result; however, it is not appropriate for a general value of p_{TP} . Following a similar logic, $\hat{\theta}_i = 0$ is obtained when at least one of the components of $\tilde{\theta}_{\mu \rightarrow i}$ among $\mu \in \mathcal{G}(i)$ takes the value 0, which is achieved at $p_{TP} = 1$ and $Y_\mu = 0$ or $p_{TP} = 0$ and $Y_\mu = 1$. The former case means that all the patients belonging to the μ -th test are negative when $Y_\mu = 0$ and $p_{TP} = 1$. In the latter case, $Y_\mu = 1$ means $Y_\mu^{(0)} = 0$ because $p_{TP} = 0$; Hence, all the patients belonging to the positive test are negative. In other words, $\hat{\theta}_i$ is always larger than zero when p_{TP} is less than 1 or more than 1. Therefore, all the patients are determined as positive under the threshold at $\hat{\theta}_i = 0$, which corresponds to $FP = 1$.

IV. IMPROVEMENT OF TRUE-POSITIVE RATE CONSIDERING FLUCTUATION OF THE ESTIMATES

The estimated Bernoulli probability $\hat{\theta}$ is a function of \mathbf{Y} , and fluctuates depending on the probabilistic observation. The quantification of the credibility of $\hat{\theta}$ helps in determining the infected patients under conditions of noisy observation data. The confidence interval is one of the guides in inference considering the input fluctuation [22]. For convenience, we introduce the following statistic:

$$\hat{\tau}_i \equiv \log \frac{\hat{\theta}_i}{1 - \hat{\theta}_i}, \quad (31)$$

which gives the MAP estimator as

$$\hat{X}_i^{\text{MAP}} = \mathbb{I}(\hat{\tau}_i > 0). \quad (32)$$

Here, we assume that the generative model has the corresponding “true value” τ_i . Following the normal theory, the 95% confidence interval of the true value of τ_i is constructed as

$$\tau_i \in [\hat{\tau}_i - 1.96\hat{\sigma}_i, \hat{\tau}_i + 1.96\hat{\sigma}_i], \quad (33)$$

where 1.96 is the 97.5% quantile of the standard normal distribution, and $\hat{\sigma}_i$ is the estimate of the standard error. We resort to the nonparametric bootstrap method to estimate the standard error [23]. We generate $b = 1, \dots, N_B$ bootstrap samples $\mathbf{Y}^{(b)} \in \{0, 1\}^M$ and $\mathbf{F}^{(b)} \in \{0, 1\}^{M \times N}$ as

$$\{y_\mu^{(b)}, \tilde{\mathbf{F}}_\mu^{(b)}\} \sim \hat{P}(y, \tilde{\mathbf{F}}), \quad (34)$$

where $\tilde{\mathbf{F}}_\mu^{(b)}$ is the μ -th row vector of $\mathbf{F}^{(b)}$ and $\hat{P}(Y, \tilde{\mathbf{F}})$ is the empirical distribution of given \mathbf{Y} and \mathbf{F} defined by

$$\hat{P}(Y, \tilde{\mathbf{F}}) = \frac{1}{M} \sum_{\nu=1}^M \delta(y - y_\nu) \delta(\tilde{\mathbf{F}} - \tilde{\mathbf{F}}_\nu). \quad (35)$$

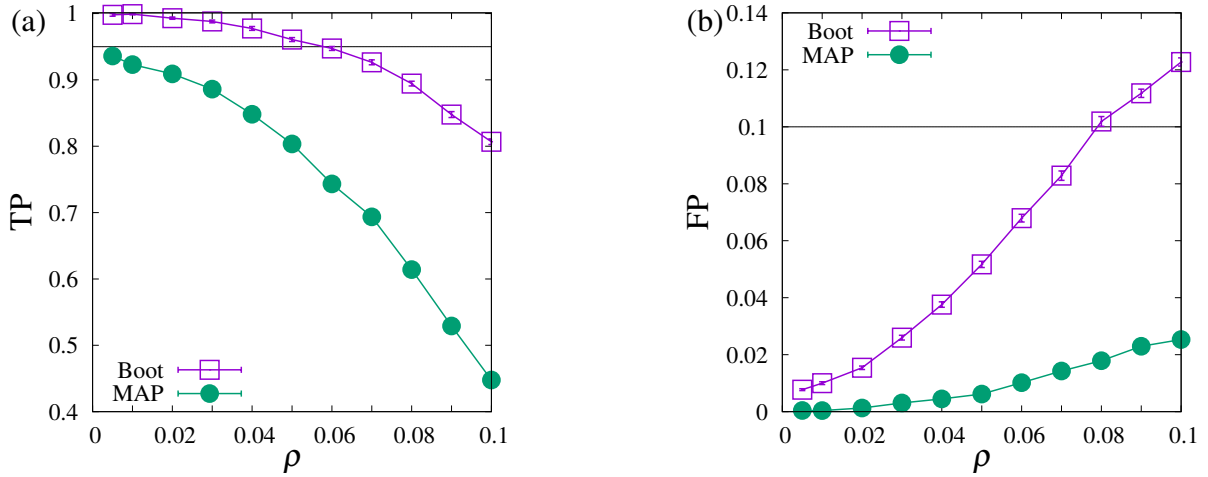


FIG. 7. ρ -dependence of (a) TP and (b) FP bootstrap estimator for $N = 1000$, $M = 500$, $N_G = 10$, $p_{TP} = 0.95$, and $p_{FP} = 0.1$.

For the construction of the confidence interval for the Bayesian point estimate, the parametric bootstrap method is another approach [24, 25] where the bootstrap samples are generated according to the posterior distribution with the point estimate. Here, we use the nonparametric approach for its simplicity.

We execute the BP algorithm for every bootstrap sample, and denote the estimate under the b -th bootstrap sample as $\hat{\tau}_i^{(b)}$. The bootstrap sample contains the same row vector of \mathbf{F} with high probability. We omit the overlapped rows to stabilize the BP algorithm. Using $\tau_i^{(b)}$ ($b = 1, \dots, N_B$), we obtain the estimate of the standard error of $\hat{\theta}_i$ as

$$\hat{\sigma}_i = \sqrt{\frac{1}{N_B - 1} \sum_{b=1}^{N_B} (\hat{\tau}_i^{(b)} - \bar{\tau}_i)^2}, \quad (36)$$

where $\bar{\tau}_i \equiv \frac{1}{N_B} \sum_{b=1}^{N_B} \hat{\tau}_i^{(b)}$ is the average over the bootstrap samples.

We define the bootstrap estimate of the i -th patient's state as

$$\hat{X}_i^{(\text{Boot})} = \mathbb{I}(\hat{\tau}_i + 1.96\hat{\sigma}_i > 0), \quad (37)$$

indicating that the patients whose confidence interval runs over the region $\tau > 0$ are regarded as infected. In comparison with the MAP estimator eq.(32), the decision threshold over which the patients are estimated as infected is lower by $1.96\hat{\sigma}_i$. Further, when $\hat{X}_i^{(\text{MAP})} = 1$, $\hat{X}_i^{(\text{Boot})} = 1$ always. Hence, eq.(37) can change the results of the patients who are determined to be non-infected using the MAP estimator. Fig.7 shows the (a) TP and (b) FP of the bootstrap estimate at $N = 1000$, $M = 500$, $N_G = 10$, $p_{TP} = 0.95$, and $p_{FP} = 0.1$. We generate $N_B = 1000$ bootstrap samples for each set of sample $\{\mathbf{Y}, \mathbf{F}, \mathbf{X}^{(0)}\}$, and each point is averaged over 100 samples. The MAP estimator cannot achieve a higher TP than p_{TP} for any ρ ; however, the bootstrap estimator improves the TP to be greater than p_{TP} . Moreover, the FP of the bootstrap estimator is higher than that of the MAP estimator; this is caused by the reduced decision threshold compared with that of the MAP estimator. However, the FP is smaller than p_{FP} for a sufficiently small ρ ; hence, I consider the bootstrap estimator as practicable. The situation is the same for other parameter regions. As an example, we show the TP and FP of bootstrap estimator at $N = 1000$, $M = 400$, $N_G = 20$, $p_{TP} = 0.95$, and $p_{FP} = 0.1$ in Fig.8.

For the intuitive understanding of the bootstrap estimator, I show examples of the bootstrap distributions of τ in Fig.9 at $N = 1000$, $M = 500$, $N_G = 10$, $p_{TP} = 0.95$, and $p_{FP} = 0.1$, where the solid line represents $\hat{\tau}$ and the two dashed lines indicate the confidence interval. This histogram was obtained from 1000 bootstrap samples; note that the confidence interval eq.(33) is not that for the bootstrap distribution. Fig.9(a) shows the bootstrap distribution of an infected patient who is judged as non-infected by the MAP estimator and as infected by the bootstrap estimator. Fig.9(b) shows the same for a non-infected patient. The patients shown in Fig.9 (a) and (b) contribute to the increase of the TP and FP of the bootstrap estimate, respectively.

Another construction method of the credible interval is the use of the bootstrap percentile as

$$\tau \in [G_B^{-1}(0.025), G_B^{-1}(0.975)], \quad (38)$$

where $G_B^{-1}(\alpha)$ is the α -percentile of the bootstrap distribution. I tried this interval for determining the infected patients. The obtained TP is comparable with the normal theory; however, the FP tends to be large compared with the interval determined by the normal theory.

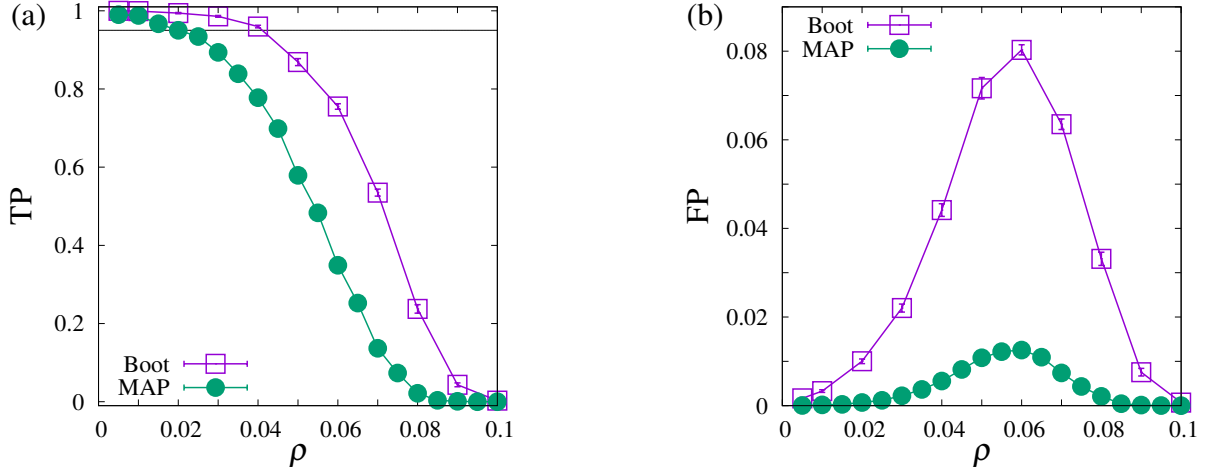


FIG. 8. ρ -dependence of (a) TP and (b) FP bootstrap estimator for $N = 1000$, $M = 400$, $N_G = 20$, $p_{TP} = 0.95$, and $p_{FP} = 0.1$.

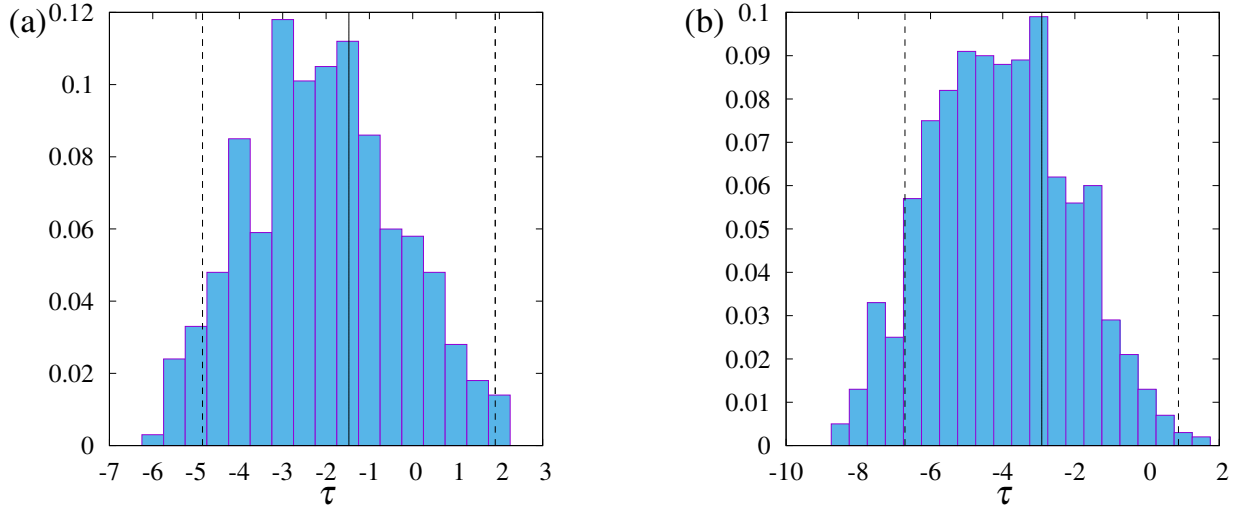


FIG. 9. Examples of bootstrap distribution at $N = 1000$, $M = 500$, $N_G = 10$, $p_{TP} = 0.95$, and $p_{FP} = 0.1$. The width of the bin is set at 0.5. The solid line and dashed lines represent $\hat{\tau}$ and the confidence interval, respectively. (a) Bootstrap distribution of τ for an infected patient where $\hat{X}_i^{(MAP)} = 0$ and $\hat{X}_i^{(Boot)} = 1$. (b) Bootstrap distribution of τ for a non-infected patient where $\hat{X}_i^{(MAP)} = 0$ and $\hat{X}_i^{(Boot)} = 1$.

V. ESTIMATION OF UNKNOWN PARAMETERS BY EXPECTATION MAXIMIZATION

In this section, we consider the estimation of the unknown parameters: prevalence ρ , TP probability p_{TP} , and FP probability p_{FP} . We construct their estimator by the maximum likelihood method, where the likelihood is given by

$$\sum_{\mathbf{X}} P(\mathbf{Y}|\mathbf{X}, p_{TP}, p_{FP})P(\mathbf{X}|\rho) = P(\mathbf{Y}|\rho, p_{TP}, p_{FP}), \quad (39)$$

and the estimators are given by

$$\hat{\rho} = \arg \max_{\rho} \ln P(\mathbf{Y}|\rho, p_{TP}, p_{FP}) \quad (40)$$

$$\hat{p}_{TP} = \arg \max_{p_{TP}} \ln P(\mathbf{Y}|\rho, p_{TP}, p_{FP}) \quad (41)$$

$$\hat{p}_{FP} = \arg \max_{p_{FP}} \ln P(\mathbf{Y}|\rho, p_{TP}, p_{FP}). \quad (42)$$

An approximation of the log-likelihood is given by the BP algorithm as Bethe free entropy [20], defined as

$$\mathcal{S} = \sum_{\mu=1}^M \ln \mathcal{Z}_{\mu} + \sum_{i=1}^N \ln \mathcal{Z}_i - \sum_{\mu} \sum_{i \in \mathcal{M}(\mu)} \ln \mathcal{Z}_{\mu i}, \quad (43)$$

where

$$\begin{aligned} \mathcal{Z}_{\mu} &\equiv \sum_{\mathbf{X}} \prod_{i \in \mathcal{M}(\mu)} m_{i \rightarrow \mu}(X_i) P(Y_{\mu} | \mathbf{X}) \\ &= U_{\mu} (1 - \tilde{q}_{\mu}) + W_{\mu} \tilde{q}_{\mu} \end{aligned} \quad (44)$$

$$\begin{aligned} \mathcal{Z}_i &\equiv \sum_{X_i} \prod_{\mu \in \mathcal{G}(i)} \tilde{m}_{\mu \rightarrow i}(X_i) \{\rho X_i + (1 - \rho)(1 - X_i)\} \\ &= \rho \prod_{\mu \in \mathcal{G}(i)} \tilde{\theta}_{\mu \rightarrow i} + (1 - \rho) \prod_{\mu \in \mathcal{G}(i)} (1 - \tilde{\theta}_{\mu \rightarrow i}) \end{aligned} \quad (45)$$

$$\begin{aligned} \mathcal{Z}_{\mu i} &\equiv \sum_{X_i} m_{i \rightarrow \mu}(X_i) \tilde{m}_{\mu \rightarrow i}(X_i) \\ &= \theta_{i \rightarrow \mu} \tilde{\theta}_{\mu \rightarrow i} + (1 - \theta_{i \rightarrow \mu})(1 - \tilde{\theta}_{\mu \rightarrow i}), \end{aligned} \quad (46)$$

and

$$\tilde{q}_{\mu} = \prod_{i \in \mathcal{M}(\mu)} (1 - \theta_{i \rightarrow \mu}). \quad (47)$$

We derive the maximum-likelihood estimator by the stationary condition of the Bethe free entropy [26]. After the calculation shown in AppendixB, we obtain

$$\hat{\rho} = \frac{1}{N} \sum_{i=1}^N \hat{\theta}_i \quad (48)$$

$$\hat{\rho}_{\text{TP}} = \frac{\frac{1}{M} \sum_{\mu=1}^M \langle \mathbb{I}(Y_{\mu} = 1, T_{\mu}(\mathbf{X}_{(\mu)}) = 1) \rangle_{\mu}}{\frac{1}{M} \sum_{\mu=1}^M \langle \mathbb{I}(T_{\mu}(\mathbf{X}_{(\mu)}) = 1) \rangle_{\mu}} \quad (49)$$

$$\hat{\rho}_{\text{FP}} = \frac{\frac{1}{M} \sum_{\mu=1}^M \langle \mathbb{I}(Y_{\mu} = 1, T_{\mu}(\mathbf{X}_{(\mu)}) = 0) \rangle_{\mu}}{\frac{1}{M} \sum_{\mu=1}^M \langle \mathbb{I}(T_{\mu}(\mathbf{X}_{(\mu)}) = 0) \rangle_{\mu}}, \quad (50)$$

where $\langle \cdot \rangle_{\mu}$ denotes the expectation of $\mathbf{X}_{(\mu)} \equiv \{X_i | i \in \mathcal{M}(\mu)\}$ according to the posterior distribution with respect to the μ -th test defined by

$$P_{\mu}(\mathbf{X}_{(\mu)} | Y_{\mu}) = \frac{1}{\mathcal{Z}_{\mu}} P(Y_{\mu} | \mathbf{X}_{(\mu)}) \prod_{i \in \mathcal{M}(\mu)} m_{i \rightarrow \mu}(X_i), \quad (51)$$

and

$$\langle \mathbb{I}(Y_{\mu} = 1, T_{\mu}(\mathbf{X}_{(\mu)}) = 1) \rangle_{\mu} = \frac{p_{\text{TP}} Y_{\mu} (1 - \tilde{q}_{\mu})}{\mathcal{Z}_{\mu}} \quad (52)$$

$$\langle \mathbb{I}(Y_{\mu} = 1, T_{\mu}(\mathbf{X}_{(\mu)}) = 0) \rangle_{\mu} = \frac{p_{\text{FP}} Y_{\mu} \tilde{q}_{\mu}}{\mathcal{Z}_{\mu}} \quad (53)$$

$$\langle \mathbb{I}(T_{\mu}(\mathbf{X}_{(\mu)}) = 1) \rangle_{\mu} = \frac{U_{\mu} (1 - \tilde{q}_{\mu})}{\mathcal{Z}_{\mu}} \quad (54)$$

$$\langle \mathbb{I}(T_{\mu}(\mathbf{X}_{(\mu)}) = 0) \rangle_{\mu} = \frac{W_{\mu} \tilde{q}_{\mu}}{\mathcal{Z}_{\mu}}. \quad (55)$$

Eqs. (49)–(50) always have trivial fixed points at 0 and 1, and to avoid these solutions, we solve following expressions:

$$f(u, v) \equiv \sum_{\mu} \frac{(2Y_{\mu} - 1)(1 - \tilde{q}_{\mu})}{\mathcal{Z}_{\mu}} = 0 \quad (56)$$

$$g(u, v) \equiv \sum_{\mu} \frac{(2Y_{\mu} - 1)\tilde{q}_{\mu}}{\mathcal{Z}_{\mu}} = 0, \quad (57)$$

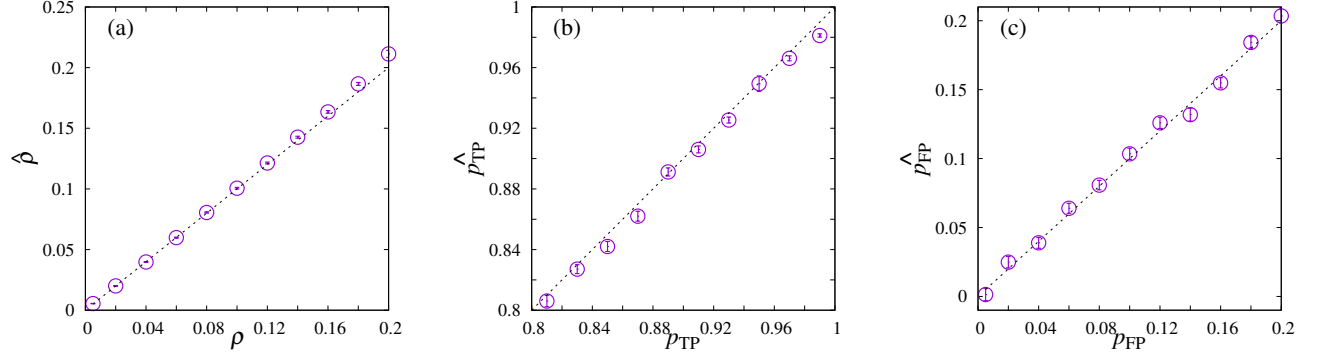


FIG. 10. Comparison between true values and estimated values of hyperparameters. The gradient of the diagonal lines is 1, and system sizes are $N = 1000$, $M = 500$, and $N_G = 10$. (a) $\hat{\rho}$ vs. ρ plot at $p_{TP} = 0.95$ and $p_{FP} = 0.1$. The parameters p_{TP} and p_{FP} are estimated by the EM method. (b) \hat{p}_{TP} vs. p_{TP} plot at $\rho = 0.1$, and $p_{FP} = 0.1$, where ρ and p_{FP} are estimated by the EM method. (c) \hat{p}_{FP} vs. p_{FP} plot at $\rho = 0.1$ and $p_{TP} = 0.95$, where ρ and p_{TP} are estimated by the EM method.

which are equivalent to eqs. (49)–(50). Note that the extremization conditions of eqs.(48)–(50) correspond to the Nishimori line [27, 28].

We calculate the infected probability of patients and the estimators of the unknown parameters by the EM method. In the E-step, the fixed points of the BP, $\{\hat{\theta}_{\mu \rightarrow i}\}$ and $\{\theta_{i \rightarrow \mu}\}$, are achieved by recursive updating under a fixed \hat{p}_{TP} , \hat{p}_{FP} and $\hat{\rho}$. In the M-step, these parameters are updated according to the extremization conditions of eqs. (48)–(50). We term this method the BP+EM algorithm, which is summarized in Algorithm 2. We solve eq.(56) and eq.(57) using the Newton method in the M-step; however, the optimization at each M-step induces algorithmic instability. Hence, we update \hat{p}_{TP} and \hat{p}_{FP} for only one step following the Newton method.

Fig.10 show the comparison between estimated parameters and true parameters at $N = 1000$, $M = 500$, and $N_G = 10$ for (a) ρ at $p_{TP} = 0.95$ and $p_{FP} = 0.1$, (b) p_{TP} at $\rho = 0.1$ and $p_{FP} = 0.1$, and (c) p_{FP} at $\rho = 0.1$ and $p_{TP} = 0.95$. The gradient of the diagonal lines is 1. Hence, the point on this line indicates that the accurate estimation of the unknown parameters is achieved. In all the figures, parameters that are not shown in the figures are also estimated simultaneously. For the entire parameter region, the M-step converges to the true parameter. The TP rate and FP rate of the BP+EM algorithm are the same as those of the BP algorithm where the parameters are known.

I note that the behavior of the BP+EM algorithm heavily depends on the initial condition of \hat{p}_{TP} and \hat{p}_{FP} . When the initial conditions of \hat{p}_{TP} and \hat{p}_{FP} are close to their true values, the BP+EM algorithm is stable; hence, the proposed method should be treated as a correction of the experimentally estimated values. The estimation of $\hat{\rho}$ is insensitive to the initial condition, which is smaller than α .

Algorithm 2 BP+EM for Bayesian group testing

Input: $Y \sim P(Y|X^{(0)})$ and F
Output: $\theta \in [0, 1]^N$

```

1: Initialize:
2:  $\{\theta_{i \rightarrow \mu}^{(0)}\} \leftarrow$  initial value from  $[0, 1]^{N \times M}$ 
    $\{\tilde{\theta}_{\mu \rightarrow i}^{(0)}\} \leftarrow$  initial value from  $[0, 1]^{M \times N}$ 
    $\{\hat{\rho}^{[0]}, \hat{\rho}_{\text{TP}}^{[0]}, \hat{\rho}_{\text{FP}}^{[0]}\} \leftarrow$  initial value from  $[0, 1]^3$ 
    $U^{[0]} \leftarrow \hat{\rho}_{\text{TP}}^{[0]}Y + (1 - \hat{\rho}_{\text{TP}}^{[0]})(\mathbf{1}_M - Y)$ ,  $W^{[0]} \leftarrow \hat{\rho}_{\text{FP}}^{[0]}Y + (1 - \hat{\rho}_{\text{FP}}^{[0]})(\mathbf{1}_M - Y)$ 
3: for  $s = 1 \dots S$  do
4:   for  $t = 1 \dots T$  do
5:     for all combinations of  $(\mu, i)$  such that  $F_{\mu i} = 1$  do
6:        $\tilde{Z}_{\mu \rightarrow i}^{(t)} \leftarrow U_{\mu}^{[s-1]} \left\{ 2 - \prod_{j \in \mathcal{M}(\mu) \setminus i} (1 - \theta_{j \rightarrow \mu}^{(t-1)}) \right\} + W_{\mu}^{[s-1]} \prod_{j \in \mathcal{M}(\mu) \setminus i} (1 - \theta_{j \rightarrow \mu}^{(t-1)})$ 
7:        $Z_{i \rightarrow \mu}^{(t)} \leftarrow \hat{\rho}^{[s-1]} \prod_{v \in \mathcal{G}(i) \setminus \mu} \tilde{\theta}_{v \rightarrow i}^{(t-1)} + (1 - \hat{\rho}^{[s-1]}) \prod_{v \in \mathcal{G}(i) \setminus \mu} (1 - \tilde{\theta}_{v \rightarrow i}^{(t-1)})$ 
8:        $\tilde{\theta}_{\mu \rightarrow i}^{(t)} \leftarrow \frac{U_{\mu}^{[s-1]}}{\tilde{Z}_{\mu \rightarrow i}^{(t)}}$ 
9:        $\theta_{i \rightarrow \mu}^{(t)} \leftarrow \frac{\hat{\rho}^{[s-1]} \prod_{v \in \mathcal{G}(i) \setminus \mu} \tilde{\theta}_{v \rightarrow i}^{(t-1)}}{Z_{i \rightarrow \mu}^{(t)}}$ 
10:    end for
11:   end for
12:   for  $i = 1 \dots N$  do
13:      $\hat{\theta}_i^{[s]} \leftarrow \frac{\hat{\rho}^{[s-1]} \prod_{\mu \in \mathcal{G}(i)} \tilde{\theta}_{\mu \rightarrow i}^{(T)}}{\hat{\rho}^{[s-1]} \prod_{\mu \in \mathcal{G}(i)} \tilde{\theta}_{\mu \rightarrow i}^{(T)} + (1 - \hat{\rho}^{[s-1]}) \prod_{\mu \in \mathcal{G}(i)} (1 - \tilde{\theta}_{\mu \rightarrow i}^{(T)})}$ 
14:   end for
15:    $\hat{\rho}^{[s]} \leftarrow \frac{1}{N} \sum_i \hat{\theta}_i^{[s]}$ 
16:   for  $\mu = 1 \dots M$  do
17:      $\tilde{q}_{\mu}^{[s]} \leftarrow \prod_{i \in \mathcal{M}(\mu)} (1 - \theta_{i \rightarrow \mu}^{(T)})$ 
18:      $Z_{\mu}^{[s]} \leftarrow U_{\mu}^{[s-1]} (1 - \tilde{q}_{\mu}^{[s]}) + W_{\mu}^{[s-1]} \tilde{q}_{\mu}^{[s]}$ 
19:   end for
20:    $f^{[s]} \leftarrow \sum_{\mu} \frac{(Y_{\mu} - (1 - Y_{\mu})) (1 - \tilde{q}_{\mu}^{[s]})}{Z_{\mu}^{[s]}}$ ,  $g^{[s]} \leftarrow \sum_{\mu} \frac{(Y_{\mu} - (1 - Y_{\mu})) \tilde{q}_{\mu}^{[s]}}{Z_{\mu}^{[s]}}$ 
21:    $G^{[s]} \leftarrow - \begin{bmatrix} \sum_{\mu} \frac{(2Y_{\mu} - 1)^2 (1 - \tilde{q}_{\mu}^{[s]})^2}{Z_{\mu}^{[s]2}} & \sum_{\mu} \frac{(2Y_{\mu} - 1)^2 (1 - \tilde{q}_{\mu}^{[s]}) \tilde{q}_{\mu}^{[s]}}{Z_{\mu}^{[s]2}} \\ \sum_{\mu} \frac{(2Y_{\mu} - 1)^2 (1 - \tilde{q}_{\mu}^{[s]}) \tilde{q}_{\mu}^{[s]}}{Z_{\mu}^{[s]2}} & \sum_{\mu} \frac{(2Y_{\mu} - 1)^2 (\tilde{q}_{\mu}^{[s]})^2}{Z_{\mu}^{[s]2}} \end{bmatrix}$ 
22:    $[\hat{\rho}_{\text{TP}}^{[s]}, \hat{\rho}_{\text{FP}}^{[s]}]^{\text{T}} \leftarrow [\hat{\rho}_{\text{TP}}^{[s-1]}, \hat{\rho}_{\text{FP}}^{[s-1]}]^{\text{T}} - G^{[s]-1} [f^{[s]}, g^{[s]}]^{\text{T}}$ 
23:    $U^{[s]} \leftarrow \hat{\rho}_{\text{TP}}^{[s]}Y + (1 - \hat{\rho}_{\text{TP}}^{[s]})(\mathbf{1}_M - Y)$ ,  $W^{[s]} \leftarrow \hat{\rho}_{\text{FP}}^{[s]}Y + (1 - \hat{\rho}_{\text{FP}}^{[s]})(\mathbf{1}_M - Y)$ 
24: end for

```

VI. HIERARCHICAL BAYES APPROACH

As another approach to estimating prevalence, we introduce the hierarchical Bayes model, where the prevalence is regarded as a hyperparameter distributed according to the hyperprior distribution

$$\phi(\rho; a, b) = \frac{\rho^{a-1} (1 - \rho)^{b-1}}{B(a, b)}, \quad (58)$$

which is the beta distribution with the hyperparameters a and b , and $B(a, b)$ is the beta function. The beta distribution is the conjugate of the Bernoulli distribution. A graphical representation of group testing for the hierarchical Bayes model is shown in Fig.11. The prior distribution of X_i under a given ρ is regarded as an ‘‘interaction’’ that is represented by a factor node I_i . We introduce additional messages $\pi_{i \rightarrow i}$, $\tilde{\pi}_{i \rightarrow i}$, $\tilde{r}_{i \rightarrow \rho}$, and $r_{\rho \rightarrow i}$ for all i , that are propagated from X_i to I_i , I_i to X_i , I_i to ρ , and ρ to I_i , respectively, as shown in Fig.11.

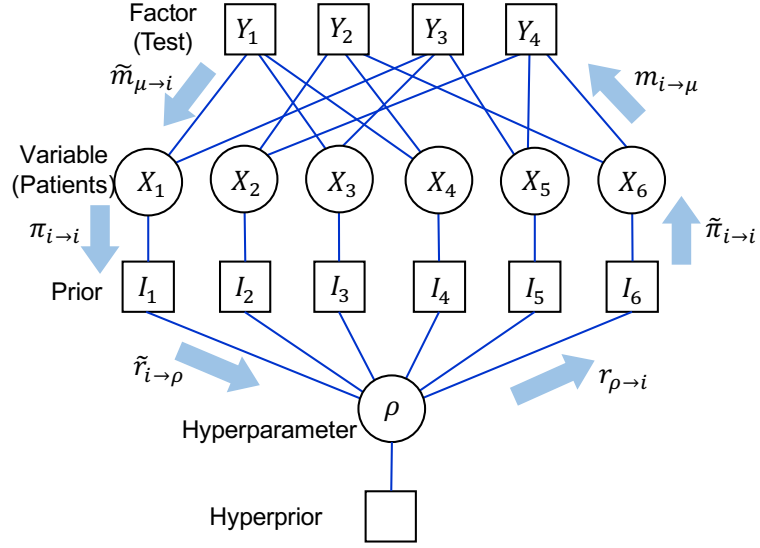


FIG. 11. Graphical representation and messages of the hierarchical Bayes model for the group testing at $N = 6$, $M = 4$, $N_G = 3$, and $N_O = 2$.

The messages propagated between the bipartite graph of Y and X are given by

$$\tilde{m}_{\mu \rightarrow i}(X_i) \propto \sum_{\mathbf{X} \setminus X_i} P(Y_\mu | \mathbf{X}) \prod_{j \in \mathcal{M}(\mu) \setminus i} m_{j \rightarrow \mu}(X_j) \quad (59)$$

$$m_{i \rightarrow \mu}(X_i) = \tilde{\pi}_{i \rightarrow i}(x_i) \prod_{v \in \mathcal{G}(i) \setminus \mu} \tilde{m}_{v \rightarrow i}(x_i), \quad (60)$$

where $\tilde{\pi}_{i \rightarrow i}$ carries the prior information to X_i . Here, we express $\tilde{\pi}_{i \rightarrow i}(x_i)$ by one parameter $\tilde{\rho}_i$, which is derived later, as

$$\tilde{\pi}_{i \rightarrow i} = \tilde{\rho}_i X_i + (1 - \tilde{\rho}_i)(1 - X_i). \quad (61)$$

Using eq.(61), the parameters $\tilde{\theta}_{\mu \rightarrow i}$ and $\theta_{i \rightarrow \mu}$ that express the messages as eqs. (14)–(15), are given by

$$\tilde{\theta}_{\mu \rightarrow i} = \frac{U_\mu}{\tilde{Z}_{\mu \rightarrow i}} \quad (62)$$

$$\theta_{i \rightarrow \mu} = \frac{\tilde{\rho}_i \prod_{v \in \mathcal{G}(i) \setminus \mu} \tilde{\theta}_{v \rightarrow i}}{Z_{i \rightarrow \mu}}, \quad (63)$$

where

$$\tilde{Z}_{\mu \rightarrow i} = U_\mu \left(2 - \prod_{j \in \mathcal{M}(\mu) \setminus i} (1 - \theta_{j \rightarrow \mu}) \right) + W_\mu \prod_{j \in \mathcal{M}(\mu) \setminus i} (1 - \theta_{j \rightarrow \mu}) \quad (64)$$

$$Z_{i \rightarrow \mu} = \tilde{\rho}_i \prod_{v \in \mathcal{G}(i) \setminus \mu} \tilde{\theta}_{v \rightarrow i} + (1 - \tilde{\rho}_i) \prod_{v \in \mathcal{G}(i) \setminus \mu} (1 - \tilde{\theta}_{v \rightarrow i}), \quad (65)$$

and U_μ and W_μ are given by eqs.(18)–(19). The messages between the variables and priors are given by

$$\pi_{i \rightarrow i}(X_i) \propto \prod_{\mu \in \mathcal{G}(i)} \tilde{m}_{\mu \rightarrow i}(x_i) \quad (66)$$

$$\tilde{\pi}_{i \rightarrow i}(x_i) = \int_0^1 d\rho \{ \rho X_i + (1 - \rho)(1 - X_i) \} r_{\rho \rightarrow i}(\rho), \quad (67)$$

and we obtain

$$\tilde{\rho}_i = \int_0^1 d\rho \rho r_{\rho \rightarrow i}(\rho). \quad (68)$$

Further, by setting

$$\pi_{i \rightarrow i}(X_i) = \pi_i X_i + (1 - \pi_i)(1 - X_i), \quad (69)$$

we obtain

$$\pi_i = \frac{\prod_{\mu \in \mathcal{G}(i)} \tilde{\theta}_{\mu \rightarrow i}}{\prod_{\mu \in \mathcal{G}(i)} \tilde{\theta}_{\mu \rightarrow i} + \prod_{\mu \in \mathcal{G}(i)} (1 - \tilde{\theta}_{\mu \rightarrow i})}, \quad (70)$$

which corresponds to the infection probability when the prior is ignored. The messages between prior I_i and the hyperparameter ρ are given by

$$\begin{aligned} \tilde{r}_{i \rightarrow \rho}(\rho) &\propto \sum_{X_i} \{\rho X_i + (1 - \rho)(1 - X_i)\} \pi_{i \rightarrow i}(X_i) \\ &= \rho \pi_i + (1 - \rho)(1 - \pi_i) \end{aligned} \quad (71)$$

$$r_{\rho \rightarrow i}(\rho) \propto \phi(\rho) \prod_{j \neq i} \tilde{r}_{j \rightarrow \rho}(\rho). \quad (72)$$

Using these messages, we can approximate the marginal distribution as

$$P(X_i) \propto \tilde{\pi}_{i \rightarrow i}(X_i) \prod_{\mu \in \mathcal{G}(i)} \tilde{m}_{\mu \rightarrow i}(X_i), \quad (73)$$

and the infection probability of X_i is estimated as

$$\hat{\theta}_i = \frac{\tilde{\rho}_i \prod_{\mu \in \mathcal{G}(i)} \tilde{\theta}_{\mu \rightarrow i}}{\tilde{\rho}_i \prod_{\mu \in \mathcal{G}(i)} \tilde{\theta}_{\mu \rightarrow i} + (1 - \tilde{\rho}_i) \prod_{\mu \in \mathcal{G}(i)} (1 - \tilde{\theta}_{\mu \rightarrow i})}. \quad (74)$$

We refer to the BP algorithm for the hierarchical Bayes model as the hierarchical BP (HBP) algorithm; its pseudocode is summarized in Algorithm 3. For HBP, we introduce an additional damping as

$$\pi_i^{(t)} \leftarrow d \pi_i^{(t)} + (1 - d) \pi_i^{(t-1)} \quad (75)$$

$$\tilde{\rho}_i^{(t)} \leftarrow d \tilde{\rho}_i^{(t)} + (1 - d) \tilde{\rho}_i^{(t-1)}. \quad (76)$$

When the infection probability of each patient can be guessed from symptoms before performing the test and has different values for each patient, we can apply the information into the prior as ρ_i . The BP algorithm for this case is obtained from the HBP by fixing the value of $\tilde{\rho}_i$ at ρ_i .

Algorithm 3 HBP for group testing**Input:** $Y \sim P(Y|X^{(0)})$ and F **Output:** $\theta \in [0, 1]^N$

```

1: Initialize:
2:    $\{\theta_{i \rightarrow \mu}^{(0)}\} \leftarrow$  initial value from  $[0, 1]^{N \times M}$ 
    $\{\tilde{\theta}_{\mu \rightarrow i}^{(0)}\} \leftarrow$  initial value from  $[0, 1]^{M \times N}$ 
    $\pi^{(0)} \leftarrow$  initial value from  $[0, 1]^N$ 
    $\tilde{\rho}^{(0)} \leftarrow$  initial value from  $[0, 1]^N$ 
3:  $U \leftarrow uY + (1-u)(\mathbf{1}_M - Y)$ ,  $W \leftarrow wY + (1-w)(\mathbf{1}_M - Y)$ 
4: for  $t = 1 \dots T$  do
5:   for all combinations of  $(\mu, i)$  such that  $F_{\mu i} = 1$  do
6:      $\tilde{Z}_{\mu \rightarrow i}^{(t)} \leftarrow U_{\mu} \left\{ 2 - \prod_{j \in \mathcal{M}(\mu) \setminus i} (1 - \theta_{j \rightarrow \mu}^{(t-1)}) \right\} + W_{\mu} \prod_{j \in \mathcal{M}(\mu) \setminus i} (1 - \theta_{j \rightarrow \mu}^{(t-1)})$ 
7:      $Z_{i \rightarrow \mu}^{(t)} \leftarrow \tilde{\rho}_i^{(t-1)} \prod_{v \in \mathcal{G}(i) \setminus \mu} \tilde{\theta}_{v \rightarrow i}^{(t-1)} + (1 - \tilde{\rho}_i^{(t-1)}) \prod_{v \in \mathcal{G}(i) \setminus \mu} (1 - \tilde{\theta}_{v \rightarrow i}^{(t-1)})$ 
8:      $\tilde{\theta}_{\mu \rightarrow i}^{(t)} \leftarrow \frac{U_{\mu}}{\tilde{Z}_{\mu \rightarrow i}^{(t)}}$ 
9:      $\theta_{i \rightarrow \mu}^{(t)} \leftarrow \frac{\tilde{\rho}_i^{(t-1)} \prod_{v \in \mathcal{G}(i) \setminus \mu} \tilde{\theta}_{v \rightarrow i}^{(t-1)}}{Z_{i \rightarrow \mu}^{(t)}}$ 
10:   end for
11:   for  $i = 1 \dots N$  do
12:      $\pi_i^{(t)} \leftarrow \frac{\prod_{\mu \in \mathcal{G}(i)} \tilde{\theta}_{\mu \rightarrow i}^{(t)}}{\prod_{\mu \in \mathcal{G}(i)} \tilde{\theta}_{\mu \rightarrow i}^{(t)} + \prod_{\mu \in \mathcal{G}(i)} (1 - \tilde{\theta}_{\mu \rightarrow i}^{(t)})}$ 
13:      $\Xi_{\rho \rightarrow i}^{(t)} \leftarrow \int_0^1 d\rho \phi(\rho) \prod_{j \neq i} \{ \rho \pi_j^{(t)} + (1 - \rho)(1 - \pi_j^{(t)}) \}$ 
14:      $\tilde{\rho}_i^{(t)} \leftarrow \frac{1}{\Xi_{\rho \rightarrow i}^{(t)}} \int_0^1 d\rho \rho \phi(\rho) \prod_{j \neq i} \{ \rho \pi_j^{(t)} + (1 - \rho)(1 - \pi_j^{(t)}) \}$ 
15:   end for
16: end for
17: for  $i = 1 \dots N$  do
18:    $\hat{\theta}_i \leftarrow \frac{\tilde{\rho}_i^{(T)} \prod_{\mu \in \mathcal{G}(i)} \tilde{\theta}_{\mu \rightarrow i}^{(T)}}{\tilde{\rho}_i^{(T)} \prod_{\mu \in \mathcal{G}(i)} \tilde{\theta}_{\mu \rightarrow i}^{(T)} + (1 - \tilde{\rho}_i^{(T)}) \prod_{\mu \in \mathcal{G}(i)} (1 - \tilde{\theta}_{\mu \rightarrow i}^{(T)})}$ 
19: end for

```

Fig.12 shows the comparison between the BP+EM algorithm and HBP algorithm for the (a) TP and (b) FP obtained by the MAP estimator at $N = 1000$, $M = 500$, $N_G = 10$, $p_{TP} = 0.95$, and $p_{FP} = 0.05$. Here, p_{TP} and p_{FP} are fixed at their true values. As shown in this figure, the TP and FP from the HBP algorithm have almost the same values as those from the BP+EM algorithm. Further, the hyperhyperparameter in the beta distribution has a small influence on the TP and FP. The beta distributions used for Fig.12 are shown in Fig.13. The mean of the beta distribution is given by $a/(a + b)$; hence, the mean of the hyperprior for $a = 0.5, b = 0.95$, $a = 1, b = 5$, and $a = 2, b = 2$ are 0.05, 1/6, and 0.5, respectively. The $a = 0.5, b = 0.95$ case describes the high probability at small values of ρ . The means of the other cases exceed the ρ -region shown in Fig.12. In particular, the mode corresponds to the mean, 0.5, in $a = b = 2$ case. Despite such ‘‘dense’’ prior, the reconstruction performance is comparable with the BP+EM method.

A. Comparison of BP+EM and HBP for finite system size

In this section, we discuss the difference between the BP+EM algorithm and HBP algorithm as estimation methods for prevalence. First, we consider the $N \rightarrow \infty$ limit, where the saddle point method can be applied to the integral of ρ in eq.(68). After the calculation shown in AppendixC, we obtain

$$\tilde{\rho}_i = \rho_i^*, \quad (77)$$

where ρ_i^* satisfies

$$\rho_i^* = \frac{1}{N-1} \sum_{j \neq i} \tilde{\theta}_j(\rho_i^*), \quad (78)$$

$$\tilde{\theta}_j(\rho) = \frac{\rho \prod_{\mu \in \mathcal{G}(j)} \tilde{\theta}_{\mu \rightarrow j}}{\rho \prod_{j \neq i} \tilde{\theta}_{\mu \rightarrow j} + (1 - \rho) \prod_{j \neq i} (1 - \tilde{\theta}_{\mu \rightarrow j})}. \quad (79)$$

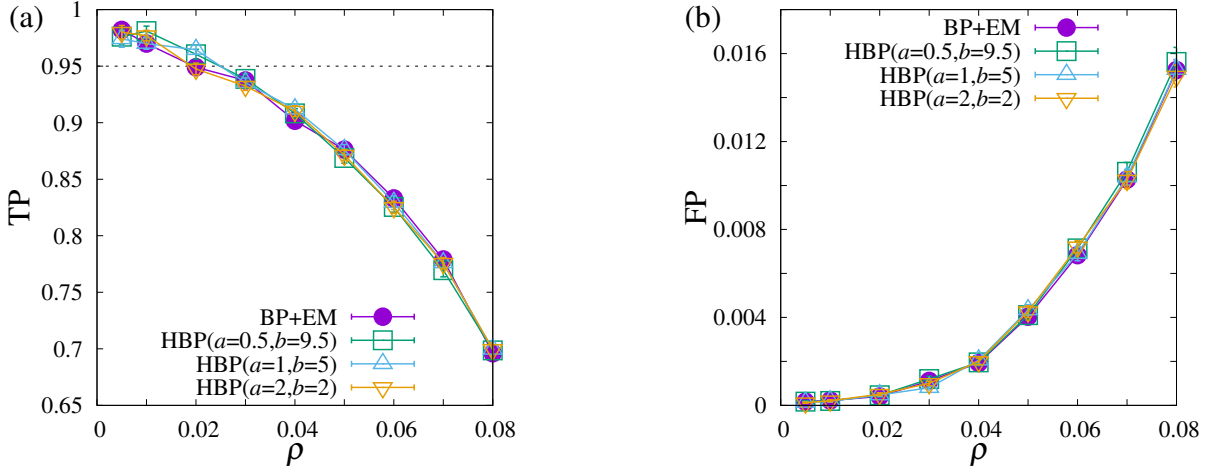


FIG. 12. Comparison of the BP+EM algorithm and HBP algorithm for (a) TP and (b) FP at $N = 1000$, $M = 500$, $N_G = 10$, $p_{TP} = 0.95$, and $p_{FP} = 0.05$. The horizontal line in (a) indicates $TP = p_{TP}$.

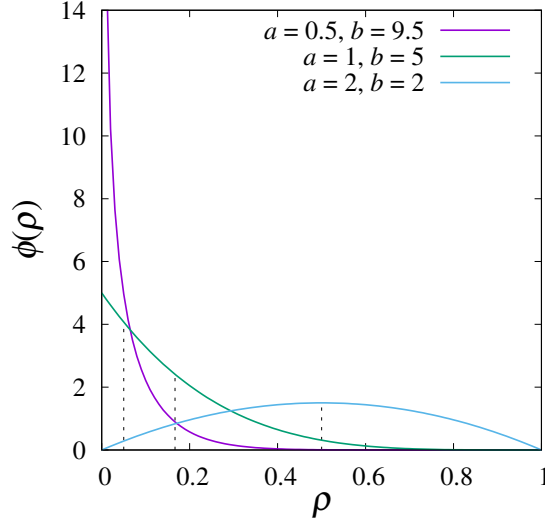


FIG. 13. Beta distributions at $a = 0.5, b = 9.5$, $a = 1, b = 5$, and $a = 2, b = 2$, which are used in Fig.12 as hyperprior. Their means are 0.05, $1/6$, and 0.5, respectively, denoted by dashed lines.

We note that eq.(78) does not depend on the hyperprior and the prevalence is estimated as $\hat{\rho} = \frac{1}{N} \sum_{i=1}^N \tilde{\rho}_i$. Comparing the estimated prevalence in the HBP algorithm with that of the BP+EM algorithm, eq.(48) shows that the difference between the two estimators is negligible at $N \rightarrow \infty$. Therefore, we compare the BP+EM and HBP algorithms by focusing on the following aspects.

: (I) Accuracy as an estimator of the prevalence for finite N

As mentioned previously, the difference between the two estimators is negligible at $N \rightarrow \infty$. However, the two estimators do not coincide with each other at finite N . We quantify the accuracy of the estimator at finite N using bias defined by

$$\text{bias} = E_{\mathbf{Y}, \mathbf{F}} [|\hat{\rho}(\mathbf{Y}, \mathbf{F}) - \rho|], \tag{80}$$

where $\hat{\rho}(\mathbf{Y}, \mathbf{F})$ denotes the estimates under given \mathbf{Y} and \mathbf{F} . An accurate estimator results in a low bias value.

: (II) Computational time

Although the mathematical forms of the estimator of prevalence are similar, the update rules in BP+EM algorithm and HBP algorithm differ from each other. The BP+EM algorithm consists of a double loop, namely the E-step for BP and the M-step for updating $\hat{\rho}$. In the HBP algorithm, the messages and the estimator are updated at the same time. The difference between these update rules influences the computational time.

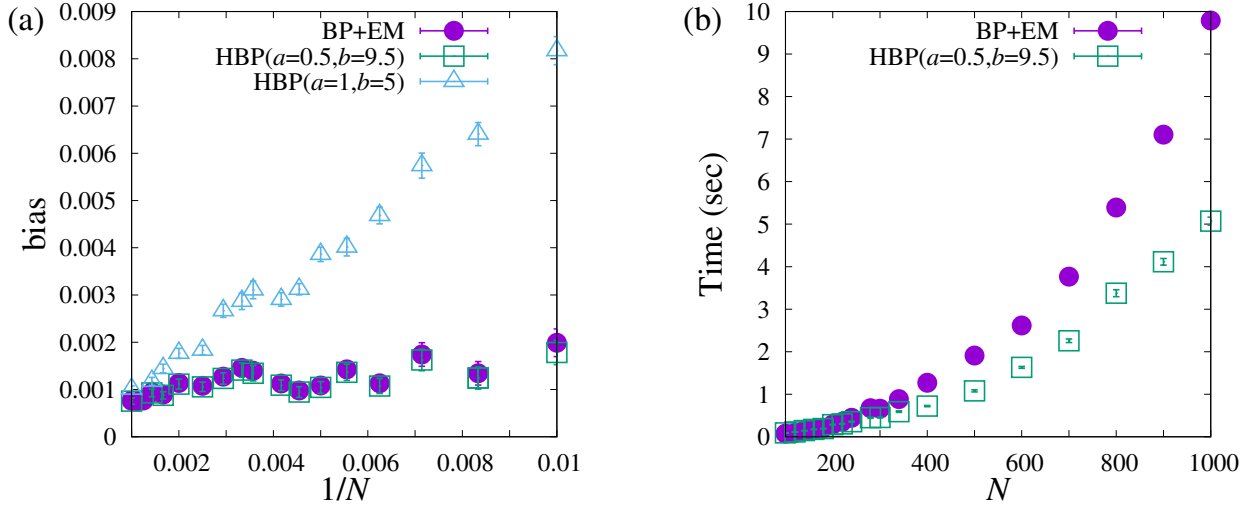


FIG. 14. (a) $1/N$ -dependence of bias and (b) N -dependence of computational time in seconds at $\alpha = 0.5$, $\rho = 0.05$, $p_{TP} = 0.99$, and $p_{FP} = 0.01$.

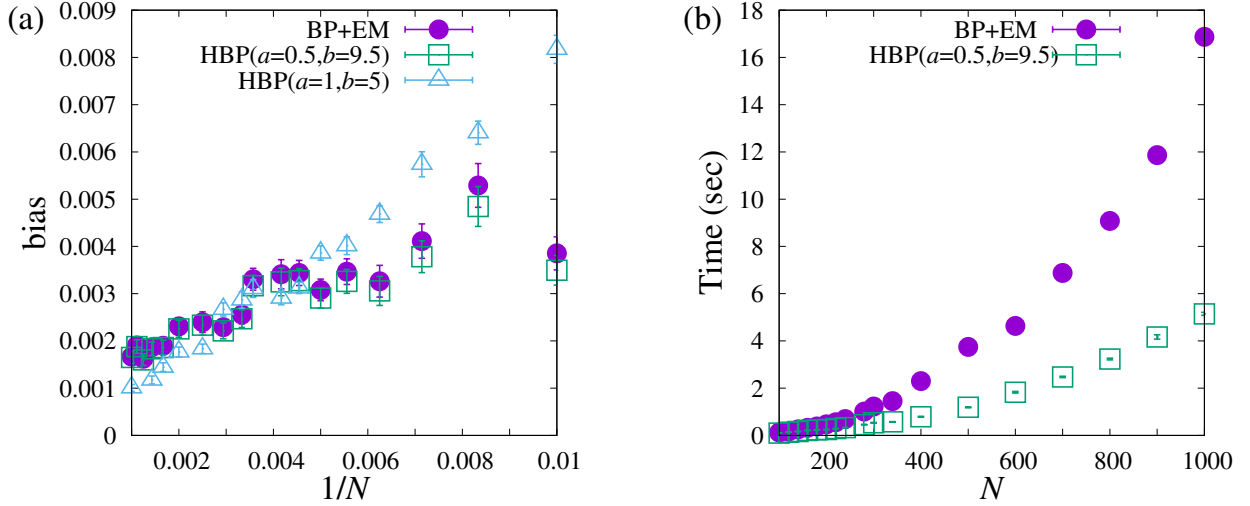


FIG. 15. (a) $1/N$ -dependence of bias and (b) N -dependence of computational time in seconds at $\alpha = 0.5$, $\rho = 0.05$, $p_{TP} = 0.95$, and $p_{FP} = 0.05$.

Fig.14 (a) and Fig.15 (a) show the N -dependence of the bias for the BP+EM and HBP algorithms at $\alpha = 0.5$, $\rho = 0.05$, $p_{TP} = 0.99$, $p_{FP} = 0.01$ (Fig.14), and $\alpha = 0.5$, $\rho = 0.05$, $p_{TP} = 0.95$, $p_{FP} = 0.05$ (Fig.15). The same 100-realization of X^0 , F , and Y were used for comparing these methods. The mean of the hyperprior at $a = 0.5$, $b = 0.95$ matches the true value of ρ . BP+EM and HBP at $a = 0.5$, $b = 0.95$ show almost the same dependency on N in bias. When a and b are not chosen to match the mean of the hyperprior, bias becomes large in finite N , but the difference in bias vanishes as $N \rightarrow \infty$.

Fig.14 (b) and Fig.15 (b) show the N -dependence of the computation time, where we fixed our experimental environment to use a single 3.5 GHz Intel Core i7 CPU. The computational time of the HBP algorithm is less than that of the BP+EM algorithm, and this priority stands out for the high-noise case, which is evident from the comparison between Fig.14 (b) and Fig.15 (b).

From these results, we consider that the choice of using the BP+EM or HBP algorithm depends on the purpose. When precise estimation of prevalence is required and there is no conception of the appropriate hyperprior in small system size, the BP+EM algorithm should be used. For quick identification of the infected patients, in particular for a large system size, the HBP algorithm is well suited to the demand.

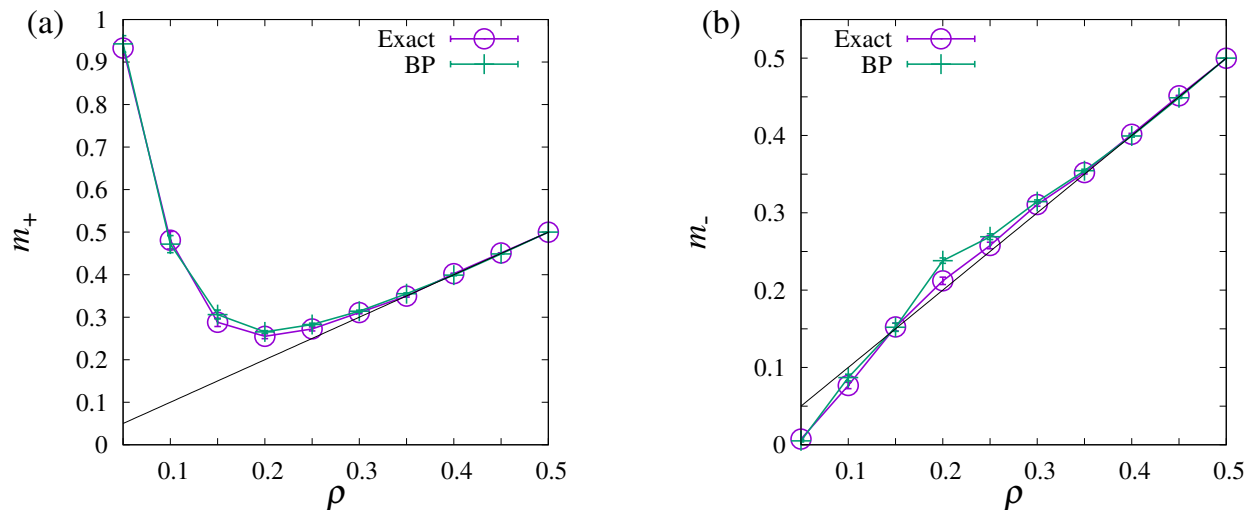


FIG. 16. ρ -dependence of (a) m_+ and (b) m_- at $N = 20$, $M = 10$ and $N_G = 10$ for exact calculation (Exact) and approximation by BP algorithm (BP). Error rates are fixed at $p_{TP} = 0.95$ and $p_{FP} = 0.02$. The gradients of solid lines are 1.

VII. SUMMARY AND DISCUSSION

In this study, we investigated the group testing problem where the test possesses finite false probabilities. We introduced the BP algorithm to evaluate the infected patients under the Bayesian inference settings. The performance of the BP algorithm, in particular for the TP rate, was improved by considering the credible interval of the point estimate assigned to each patient. Our approach used the bootstrap distribution to estimate the interval. The unknown parameters in the model, particularly prevalence, can be estimated using the EM method and hierarchical Bayes modeling. We compared these methods and formulated a guide for practical usage.

We concentrated on the pooling matrix randomly constructed under the column-wise and row-wise constraints specified by N_G and N_O . The adaptive procedure of group testing was also examined, where the pooling for the next stage was sequentially designed by considering the output of the test in the previous stage [29–31]. An extension of our BP and HBP algorithms to the adaptive setting is a promising way to explore more efficient pooling and test scheduling.

The MATLAB code used in this study is distributed on GitHub <https://github.com/AyakaSakata/GroupTesting>.

ACKNOWLEDGMENTS

This work was motivated by non-face-to-face discussions with Yukito Iba during our remote work owing to COVID-19. First, I thank him for our fruitful discussions and his visionary comments. Further, I thank Koji Hukushima, Yoshiyuki Ninomiya, Tomoyuki Obuchi, and Satoshi Takabe for helpful comments and discussions. This research was partially supported by a Grant-in-Aid for Scientific Research 19K20363 from the Japanese Society for the Promotion of Science (JSPS) and JST PRESTO Grant Number JPMJPR19M2, Japan.

Appendix A: Comparison between exact calculation and approximation by BP algorithm

To check the accuracy of the approximation by the BP algorithm, we perform exact calculation of the marginalized posterior distribution at $N = 20$, and compare it with the BP algorithm. Fig.16 shows (a) m_+ and (b) m_- at $N = 20$, $M = 10$, $N_G = 10$, $p_{TP} = 0.95$, and $p_{FP} = 0.02$, calculated by sampling all possible configurations in $X \in \{0, 1\}^N$ (Exact) and the BP algorithm (BP). The gradients of the solid lines are 1. The behaviors m_+ and m_- derived by these two methods are similar to each other, and in particular, the tendency $m_+ \rightarrow \rho$ and $m_- \rightarrow \rho$ as ρ increases is observed as discussed in Section III.

Appendix B: Derivation of maximum-(approximated) likelihood estimator

The derivative of \mathcal{S} with respect to ρ , p_{TP} , and p_{FP} is given by

$$\begin{aligned}\frac{\partial}{\partial \rho} \mathcal{S} &= \sum_i \frac{\partial}{\partial \rho} \ln \mathcal{Z}_i \\ &= \sum_i \frac{\prod_{\mu \in \mathcal{G}(i)} \tilde{\theta}_{\mu \rightarrow i} - \prod_{\mu \in \mathcal{G}(i)} (1 - \tilde{\theta}_{\mu \rightarrow i})}{\mathcal{Z}_i} \\ &= \frac{\sum_i \theta_i}{\rho} - \frac{\sum_i (1 - \theta_i)}{1 - \rho}\end{aligned}\tag{B1}$$

$$\begin{aligned}\frac{\partial}{\partial p_{\text{TP}}} \mathcal{S} &= \sum_{\mu} \frac{\partial}{\partial p_{\text{TP}}} \ln \mathcal{Z}_{\mu} \\ &= \sum_{\mu} \frac{Y_{\mu}(1 - \tilde{q}_{\mu}) - (1 - Y_{\mu})(1 - \tilde{q}_{\mu})}{\mathcal{Z}_{\mu}} \\ &= \frac{\sum_{\mu} \langle \mathbb{I}(Y_{\mu} = 1, T_{\mu}(\mathbf{X}) = 1) \rangle_{\mu}}{p_{\text{TP}}} - \frac{\sum_{\mu} \langle \mathbb{I}(Y_{\mu} = 0, T_{\mu}(\mathbf{X}) = 1) \rangle_{\mu}}{1 - p_{\text{TP}}}\end{aligned}\tag{B2}$$

$$\begin{aligned}\frac{\partial}{\partial p_{\text{FP}}} \mathcal{S} &= \sum_{\mu} \frac{\partial}{\partial p_{\text{FP}}} \ln \mathcal{Z}_{\mu} \\ &= \sum_{\mu} \frac{Y_{\mu} \tilde{q}_{\mu} - (1 - Y_{\mu}) \tilde{q}_{\mu}}{\mathcal{Z}_{\mu}} \\ &= \frac{\sum_{\mu} \langle \mathbb{I}(Y_{\mu} = 1, T_{\mu}(\mathbf{X}) = 0) \rangle_{\mu}}{p_{\text{FP}}} - \frac{\langle \mathbb{I}(Y_{\mu} = 0, T_{\mu}(\mathbf{X}) = 0) \rangle_{\mu}}{1 - p_{\text{FP}}},\end{aligned}\tag{B3}$$

respectively. Solving eqs. (B1)–(B3) under the condition that they are zero, we obtain the extremization conditions in eqs.(48)–(50).

Appendix C: Estimated value of the prevalence in hierarchical Bayes model at $N \rightarrow \infty$

Substituting eq.(72) into eq.(68), we obtain the following expression.

$$\tilde{\rho}_i = \frac{\int d\rho \rho \phi(\rho) \exp \left[N \left\{ \frac{1}{N} \sum_{j \neq i} \log \{ \rho \pi_i + (1 - \rho)(1 - \pi_i) \} \right\} \right]}{\int d\rho \phi(\rho) \exp \left[N \left\{ \frac{1}{N} \sum_{j \neq i} \log \{ \rho \pi_i + (1 - \rho)(1 - \pi_i) \} \right\} \right]}.\tag{C1}$$

Applying the saddle point method, we obtain

$$\tilde{\rho}_i = \rho_i^*,\tag{C2}$$

where ρ_i^* satisfies

$$\frac{1}{N} \sum_{j \neq i} \frac{\pi_i - (1 - \pi_i)}{\rho_i^* \pi_i + (1 - \rho_i^*)(1 - \pi_i)} = 0.\tag{C3}$$

From eqs. (70) and (79), eq.(C3) is transformed as

$$\frac{1}{N} \sum_{j \neq i} \frac{\tilde{\theta}_j(\rho_i^*)}{\rho_i^*} = \frac{1}{N} \sum_{j \neq i} \frac{1 - \tilde{\theta}_j(\rho_i^*)}{1 - \rho_i^*},\tag{C4}$$

and we obtain eq.(78) by transforming eq.(C4) with respect to ρ_i^* .

- [2] D.-Z. Du and F. K. Hwang: *Combinatorial Group Testing and Its Applications* (World Scientific, 2000).
- [3] M. Sobel and P. A. Groll: *Bell System tech. J.* **28** (1959) 1179.
- [4] J. Mano, Y. Yanaka, Y. Ikezu, M. Onishi, S. Futo, Y. Minegishi, K. Ninomiya, Y. Yotsuyanagi, F. Spiegelhalter, H. Akiyama, R. Teshima, A. Hino, S. Naito, T. Koiwa, R. Takabatake, S. Furui, and K. Kitta: *J. Agric. Food Chem.* **59** (2011) 6856.
- [5] J. K. Wolf: *IEEE Transactions on Information Theory* **31** (1985) 185.
- [6] H. G. O. Katona: in *A Survey of Combinatorial Theory*, ed. N. J. Srivastava (North-Holland, 1973), Chap. 23, pp. 285–308.
- [7] E. J. Candes and T. Tao: *IEEE Transactions on information theory* **51** (2005) 4203.
- [8] D. L. Donoho: *IEEE Transactions on information theory* **52** (2006) 1289.
- [9] G. K. Atia and V. Saligrama: *IEEE Transaction on Information Theory* **58** (2012) 1880.
- [10] D. Sejdinovic and O. Johnson: 48th Annual Allerton Conference on Communication, Control, and Computing (Allerton), 2010, pp. 998 – 1003.
- [11] Y. Cheng. A statistical method of batch screening entering population from abroad by stages and groups in COVID-19 nucleic acid testing. <https://doi.org/10.1101/2020.04.02.20050914>, 2020.
- [12] C. Mentus, M. Romeo, and C. DiPaola. Analysis and Applications of Non-Adaptive and Adaptive Group Testing Methods for COVID-19. <https://doi.org/10.1101/2020.04.05.20050245>, 2020.
- [13] N. Sinnott-Armstrong, D. Klein, and H. Brendan. Evaluation of Group Testing for SARS-CoV-2 RNA. <https://doi.org/10.1101/2020.03.27.20043968>, 2020.
- [14] E. Knill, A. Schliep, and C. D Torney: *Journal of Computational Biology* **3** (1996) 395.
- [15] L. Zou, F. Ruan, M. Huang, L. Liang, H. Huang, Z. Hong, J. Yu, M. Kang, Y. Song, J. Xia, Q. Guo, T. Song, J. He, H.-L. Yen, M. Peiris, and W. Jie: *The New England Journal of Medicine* **382** (2020) 1177.
- [16] M. Mézard, M. Tarzia, and C. Toninelli: *Journal of Physics: Conference Series* **95** (2008) 012019.
- [17] K. H. Thompson: *Biometrics* **18** (1962) 568.
- [18] M. Sobel and R. M. Elashoff: *Biometrika* **62** (1975) 181.
- [19] R. Brookmeyer: *Biometrics* **55** (1995) 608.
- [20] M. Mézard and A. Montanari: *Information, physics, and computation* (Oxford University Press, 2009).
- [21] J. T. Parker, P. Schniter, and V. Cevher: *IEEE Transaction on Signal Processing* **62** (2014) 5839 .
- [22] T. Hastie, R. Tibshirani, and M. Wainwright: *Statistical Learning with Sparsity: The Lasso and Generalizations* (Chapman & Hall, 2015).
- [23] B. Efron and R. Tibshirani: *An Introduction to the Bootstrap* (Chapman & Hall, 1993).
- [24] N. L. Hjort: *Bayesian and Empirical Bayesian Bootstrapping* (1991).
- [25] B. Efron: *The Annals of Applied Statistics* **6** (2012) 1971.
- [26] F. Krzakala, M. Mézard, F. Sausset, Y. Sun, and L. Zdeborová: *Journal of Statistical Mechanics: Theory and Experiment* **2012** (2012) P08009.
- [27] Y. Iba: *J. Phys. A: Math. Gen.* **32** (1999) 3875.
- [28] H. Nishimori: *Statistical Physics of Spin Glasses and Information Processing: An Introduction* (Clarendon Pr, 2001).
- [29] M. Sobel and P. A. Groll: *Bell Labs Technical Journal* **38** (1959) 1179.
- [30] M. Sobel and P. A. Groll: *Technometrics* **8** (1966) 631.
- [31] L. Baldassini, O. Johnson, and M. Aldridge: *IEEE International Symposium on Information Theory*, 2013, pp. 2676–2680.